THE UNIVERSITY OF SOUTH ALABAMA
COLLEGE OF ENGINEERING

HYDRODYNAMIC MODELING OF RESIDENCE, EXPOSURE, AND
FLUSHING TIME RESPONSE TO RIVERINE DISCHARGE IN MOBILE
BAY, ALABAMA

BY

Christian D. Marr

A Thesis

Submitted to the Graduate Faculty of the
University of South Alabama
in partial fulfillment of the
requirements for the degree of

Master of Science

in

Civil Engineering

July 2013

Approved: Date:

Chair of Thesis Committee: Dr. Bret M. Webb

Committee Member: Dr. Kevin D. White

Committee Member: Dr. Kyeong Park

Chair of Department: Dr. Kevin D. White

Director of Graduate Studies: Dr. Thomas G. Thomas

Dean of Graduate School: Dr. B. Keith Harrison

HYDRODYNAMIC MODELING OF RESIDENCE, EXPOSURE, AND
FLUSHING TIME RESPONSE TO RIVERINE DISCHARGE IN MOBILE
BAY, ALABAMA

A Thesis

Submitted to the Graduate Faculty of the
University of South Alabama
in partial fulfillment of the
requirements for the degree of

Master of Science

in

Civil Engineering

by
Christian D. Marr
B.S., University of South Alabama, 2010
M.S.C.E., University of South Alabama, 2013
July 2013

ACKNOWLEDGMENTS

TABLE OF CONTENTS

Page

LIST OF TABLES

LIST OF FIGURES

ABSTRACT

Marr, Christian D., M.S., University of South Alabama, July 2013. Hydrodynamic Modeling of Residence, Exposure, and Flushing Time Response to Riverine Discharge in Mobile Bay, Alabama. Chair of Committee: Dr. Bret M. Webb

Measurements of hydrodynamic timescales (e.g. residence, exposure, and flushing time) generally describe the physical mass transport of particles within a water body. These measures' response and spatial variability to tides, riverine discharge, and local meteorology are investigated by performing Advanced Circulation 2-dimensional depth integrated model simulations of Mobile Bay, Alabama, a shallow, drowned river-valley estuary located on the northeastern coast of the Gulf of Mexico. Hydrodynamic model output is utilized by a Lagrangian particle tracking model to predict the trajectories of more than 30,000 discrete particles throughout the study area. Hydrodynamic timescales are estimated and analyzed based on these results. Spatially averaged timescales generally range between 4 and 130 days depending on the magnitude of riverine discharge and local meteorology. Synthesized results suggest average to excellent flushing throughout much of Mobile Bay, and relatively poor flushing along the eastern shoreline, the mid-section of Bon Secour Bay, and in some areas of the Mobile-Tensaw Delta.

INTRODUCTION

The United States' Gulf Coast has been demonstrated to be highly vulnerable to both natural and man-made environmental disasters, as hurricanes and an oil spill have devastated parts of this region in recent years. To date, thorough studies on a vast part of these coastlines is limited, and the potential degree of damage caused by these disasters is in some cases unknown. For this reason, there is an ever-growing need for further research into the natural behavior of the coastal processes that affect this fragile ecosystem.

High population density and urban development often dominate coastal regions not only in the United States, but also worldwide. Accessibility and an abundance of resources, such as food and water, have long made coastal regions appealing to human beings. In 2003, approximately 3 billion people, about one-half the world's population, lived within 200 kilometers of a coastline and by 2025, that figure will likely double (Creel 2003). Civil engineers are regularly challenged with the task of proper planning and efficient development of these regions so that minimal negative impacts occur to an area and its surrounding environment. It is inevitable, however, that

ecosystems will be affected as the human population continues to grow.

Therefore, characterization of coastal processes that impact or are impacted

by urban growth around these regions is essential to effective engineering

practice, as well as resource management.

The measurement of residence time in bays and estuaries is of particular

interest due to its extensive range of applications across various engineering

and scientific disciplines. Residence time is a measure of water-mass

retention within a specific boundary. Measurements of residence time are

extremely useful in determining water contamination and nutrient levels,

distributions of organisms, and their spatio-temporal variations in bays and

estuaries (Aikman and Lanerolle 2005). It can show the rate at which river

freshwater is flushed out of an estuary, and therefore can be used to estimate

the rate of removal of a pollutant carried by the freshwater (Huang and

Spaulding 2002). Boynton et al. (1995) argue that residence time is such an

important attribute that it should be the basis for comparative analyses of

ecosystem-scale nutrient budgets.

Terminology

Terminology related to residence time of estuaries is somewhat

ambiguous, and investigators have used an assortment of definitions to

describe the rate of removal and fate of contaminants in coastal water bodies.

Residence time is defined as how long a fluid parcel starting at a specific

location within a discrete region, will take to leave it through one of the region boundaries (Figure 1). Estuarine physicists (e.g. Ketchum 1950; Cameron and Pritchard 1963; Dyer 1973) have used the term "residence time" of water to express many different concepts, such as: the time it takes to flush an estuary; the time that river water spends in an estuary; the time it takes for the estuarine water to be renewed; the time it takes for pollutants to decrease by a factor of 1/e; and the time it takes for river water to exit an estuary. These definitions can be confusing, because they do not address the same processes; therefore, they yield different results (Wolanski et al. 1984).

Many terms are often confused with residence time (e.g. freshwater transit time, exposure time, age, renewal time, and flushing time). While these terms can be described as complementary or related to measurements of residence time, it is important to introduce accurate definitions to avoid misunderstandings. The term residence time is often used in estuarine literature to refer to the average freshwater transit time; however, freshwater transit time is a more precise term for a type of residence time (that of freshwater, starting from the head of the estuary), whereas residence time (Figure 1) is a more general term that must be clarified by specifying the material and starting distribution (Sheldon and Alber 2002).
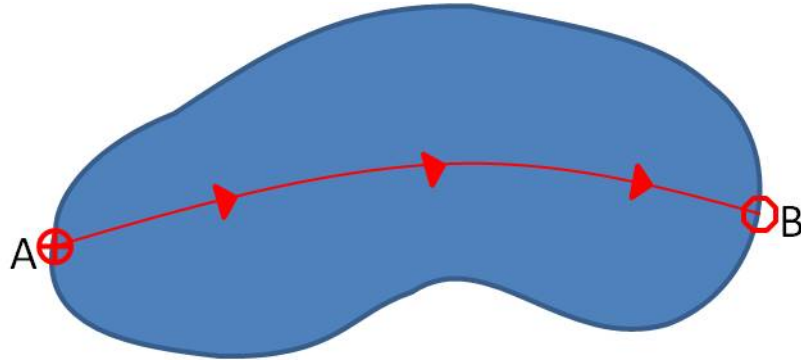
Figure 1: Illustrated depiction of a particle's residence time in a system on a 2-dimensional (2D) plane. The system is defined by the blue area; Points A and B represent the entry and exit points of the particle from the system, respectively; and the red arrows and line depict the particle trajectory.

A discrete water parcel may leave a domain during an ebb tide and return to that domain during a flood tide several times over consecutive tidal cycles. This behavior can be expressed by the measurement of exposure time (Figure 2). Exposure time is defined as the accumulated time spent by water parcels in a control domain, whereas the residence time is the time needed for a discrete water parcel to leave the domain for the first time (Zimmerman 1976).
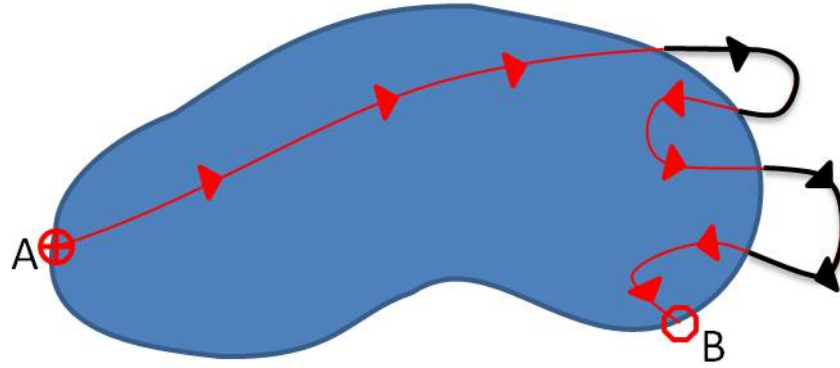
Figure 2: Illustrated depiction of a particle's exposure time in a system on a 2D plane. The system is defined by the blue area; Points A and B represent the entry and exit points of the particle from the system, respectively; the red arrows and line depict the particle trajectory; and the black line depicts where the particle has left the system but returned to the system during the tracking time.

Related to residence time in bays and estuaries, age is defined as the time a particle remains in a predefined system/region before exiting the system (Figure 3); therefore, age is unique to each discrete particle and discrete locations within the system. The concepts of age and residence times are complementary to each other so that relative to a common spatial location within a region. The transit time is the sum of age and residence time, and therefore representing the total time that a particle/fluid parcel spends (between entrance and exit) in this region (Zimmerman 1976).
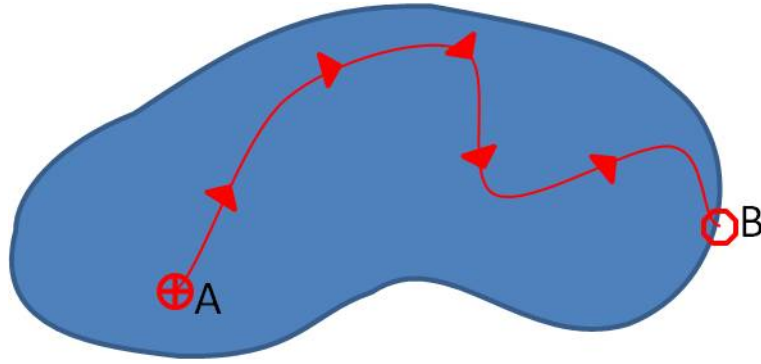
Figure 3: Illustrated depiction of a particle's age in a system on a 2D plane. The system is defined by the blue area; Points A and B represent the particle position in the system when particle tracking begins and ends, respectively; and the red arrows and line depict the particle trajectory.

Flushing time (Figure 4) is calculated as the amount of time required to reduce some initial concentration to 1/e (where, e=2.71828 and therefore, 1/e ~0.37) of its initial value (Ketchum 1950; Dyer 1973). Flushing of an estuary is usually considered relative to inflow; that is, replacing the water present at some initial time with contributions of new freshwater and new seawater (Sheldon and Alber 2006). Evaporation represents a loss of freshwater that should be subtracted from the sources, but if net precipitation minus evaporation is much smaller than the other sources of freshwater, they can both be ignored (Solis and Powell 1999; Hagy et al. 2000).

$$C_0 = 100\%$$
$$t=t_0$$

$$C_{flush} = 36.79\% \ (1/e)$$
$$t=t_{flush}$$
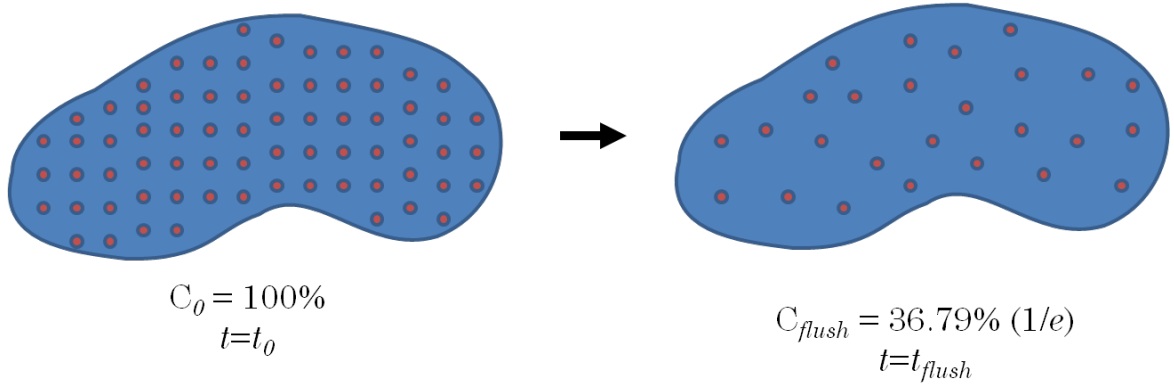
Figure 4: Illustrated depiction of a particle's flushing time in a system on a 2D plane. The system is defined by the blue area; particle positions are represented by red dots.

Analytical Methods

The measurement of residence time has been predominantly based on empirical studies using tracers (e.g. salinity or dye), very simple box models, and 1- and 2-dimensional models, such as the freshwater fraction and tidal prism methods (Miller and McPherson 1991; Signell and Butman 1992; Hagy et al. 2000; Sheldon and Alber 2002, 2006). Tracer studies are costly and often impractical considering the expertise of local managers (Kuo et al. 2005). Freshwater fraction and tidal prism methods have been applied to a variety of coastal systems to describe a range of coastal processes, such as flushing capacities and water quality in small coastal basins (Miller and McPherson 1991; Signell and Butman 1992; Hagy et al. 2000; Sheldon and Alber 2002, 2006; Kuo et al. 2005). However, with the continued advancement of these methods and technology, experts propose the use of sophisticated hydrodynamic models (Burwell et al. 2000; Shen and Haas

2004; Huang 2007; Meyers and Luther 2008) that solve a complex system of equations to represent the circulation dynamics, where applicable.

The freshwater fraction method (Dyer 1973) includes flushing by freshwater inflow (Sheldon and Alber 2006) and has been criticized for excluding flushing by seawater (Knoppers et al. 1991; Guo and Lordi 2000; National Research Council 2000). However, this is accounted for implicitly because the average estuary salinity used in the calculation reflects all the processes that bring seawater into the estuary, including gravitational circulation and tidal processes (Sheldon and Alber 2006). It should be noted that estimates calculated using the freshwater fraction method are dependent on the investigators assumed average estuary salinity. Tidal prism models are based on flushing by flood tide inflow (i.e. tidal flushing) and ignore seawater inflow due to gravitational circulation. The concept of tidal flushing has been applied to estimate the physical mass transport process for small coastal basins (Ketchum 1951; Kuo and Neilson 1988; Miller and McPherson 1991; Sanford et al. 1992; Kuo et al. 2005). Freshwater fraction methods are appropriate for estuaries with relatively high freshwater inflow, and tidal prism methods are applicable in situations such as well-mixed lagoons where freshwater inflow is low and gravitational circulation is weak (Sheldon and Alber 2006).

The choice of which method to apply is typically dependent on the need for precision in calculation and the investigator's experience with using complex

numerical modeling software. The physical characteristics of a water body (e.g. depth, volume, surface area, and average daily inflow) can also dictate the appropriate choice of method. Simple models, like the low-order box models (Miller and McPherson 1991; Signell and Butman 1992; Hagy et al. 2000; Sheldon and Alber 2002; Sheldon and Alber 2006), are adequate if the concern is for the average condition in an entire bay or estuary, but they greatly underestimate, or do not address, the residence times associated with smaller regions having restricted circulation, such as urban harbors and embayments (Aikman and Lanerolle 2005). These simple box steady-state methods may be accurate enough for scaling or for gross comparisons, but these assumptions are not always reasonable (Sheldon and Alber 2006). For this reason, in addition to advancements in existing models, residence time calculations have been trending towards the use of complex hydrodynamic numerical models.

<u>Modeling Methods</u>

The advancement of hydrodynamic computer models has enhanced the ability to calculate residence time estimates with better resolutions (Burwell et al. 2000; Shen and Haas 2004; Huang 2007; Meyers and Luther 2008) than those from the simple box model method (Miller and McPherson 1991; Signell and Butman 1992; Hagy et al. 2000; Sheldon and Alber 2002). Model outputs, with their high spatial and temporal resolutions, can be used to achieve more

refined estimates of residence time for the computational regions of application and also to determine the physical factors most affecting their value and spatial distributions (Aikman and Lanerolle 2005). These models solve a system of equations describing conservation of mass, momentum, heat and salinity for a given grid and are capable of producing estimations for important flow-field information, such as water surface elevation, temperature, salinity, and flow velocity distributions. Applications of the numerical models to a variety of coastal settings all produce circulation predictions, which seem quite realistic when compared to the available data/theory (Blumberg and Mellor 1987).

<u>Particle Tracking Methods</u>

In general, two distinct methods have been widely used when calculating residence times with numerical particle tracking model outputs: the Eulerian approach (tracer/concentration), and the Lagrangian particle path/trajectory approach. The Eulerian method is a concentration-based modeling effort, where the bay can be initialized at 100 percent concentration in a numerical model and flushing time can be defined as the time it takes for each cell's vertically integrated normalized concentration to fall below 1/e of the original vertically integrated concentration (Burwell et al. 2000). The Lagrangian approach is a particle tracking method where each model grid cell is initialized with a discrete particle density per grid cell that is uniform over

10

the water column and located on the cell center. The flushing time is taken as the time it takes for each grid cell to fall below 1/e of the original normalized daily value without regard to which grid cell a particle started in or the position of the particles in a given grid cell.

The Eulerian approach is ideally suited to simulate substance distributions in an entire bay or estuary and the Lagrangian for simulation of the transport of a substance locally in various sub-domains within a bay or estuary (Aikman and Lanerolle 2005). Cross-calibration tests between the two approaches are often necessary, so that the particle paths are consistent with the dynamics of a passive tracer patch (Blumberg et al. 2004). There has been some debate (Burwell et al. 2000) whether the Eulerian and Lagrangian approaches are comparable, which may not always be the case. Eulerian calculations for dissolved constituents usually treat the water-land boundary (including the bottom) as reflective, while for particulate materials this boundary is often treated as adsorptive (Aikman and Lanerolle 2005).

<u>Model Output Utilization</u>

Based on the output from these hydrodynamic models, residence time can be calculated using various methods. Huang and Spaulding (2002) utilize model output with the freshwater fraction method (Lauff 1967; Dyer 1973; Swanson and Mendelsohn 1996) to determine estuarine response to freshwater input. It should be noted that this approach results in the

11

freshwater transit time of the study area, which is defined as the rate at which river freshwater is flushed out of an estuary (Thomann and Muller 1987). As previously stated, freshwater transit times give estimations for the residence time of freshwater (and substances dissolved in that freshwater) starting from the head of the estuary. This technique provides an estimation of the timescale over which contaminants, or other materials released in the estuary, are removed from the system (Huang and Spaulding 2002).

When using the freshwater fraction method, a previously calibrated hydrodynamic model determines the accumulated freshwater volume in the bay by multiplying the volume of the grid with the freshwater fraction. Residence time can then be calculated by dividing the total accumulated freshwater volume by the average freshwater input for the study period. This method does not require the coupling of a constituent transport model or expensive dye release experiments (Huang and Spaulding 2002). Comparisons of model outputs with available observation data, such as water surface elevation are necessary to verify model fidelity.

The continued development of sophisticated hydrodynamic models allows an investigator to include or exclude various forcing functions to determine the response of an estuary to multiple parameters. These models can be used to examine the response of a particular estuarine parameter (e.g. residence time) to a specific dynamic forcing function (e.g. river flow) while keeping other forcing constant (e.g. winds and tides) (Huang and Spaulding 2002).

Some of the advantages of using hydrodynamic models are: (*i*) no particular model/behavior for residence times is assumed and a more fundamental approach for calculating them is adopted; (*ii*) due to high spatio-temporal resolution of model output, the spatio-temporal behavior of residence times can be investigated in domains of arbitrary size; and (*iii*) several numerical methods can be used with model output to calculate and compare residence times (Aikman and Lanerolle 2005). Hydrodynamic models are widely accepted as an important tool for describing estuarine circulation, and have been successfully applied (Burwell et al. 2000; Shen and Haas 2004; Huang 2007; Meyers and Luther 2008) to the determination of residence times in coastal water bodies.

Study Area

Mobile Bay is a shallow drowned river-valley estuary located on the northeastern coast of the Gulf of Mexico (Figure 5), and receives freshwater discharge primarily from the Alabama and Tombigbee rivers within a drainage basin of 115,467 km^2 (Quinn et al. 1986). The bay is relatively large, approximately 50 km in length (north-south) and 14-34 km in width (east-west), has a surface area of 985 km^2, and the estuarine volume is estimated to be 3.2 billion cubic meters (Quinn et al. 1986; Dinnel et al. 1990). The mean depth in Mobile Bay is approximately 3 meters, and a dredged navigation channel is maintained at 15 meters depth along the entire length

of the estuary (Figure 6). Its connections to the Gulf of Mexico and Mississippi Sound, Main Pass and Pass aux Herons (Figure 5), respectively, are comparatively narrow and shallow (Schroeder and Wiseman 1986). Estuarine-gulf exchange is characterized by a diurnal tide with a mean range at Dauphin Island and the Mobile State Docks of 0.36 and 0.5 meters, respectively. On average Main Pass accommodates for more estuary-gulf exchange than Pass aux Herons (approximately 85% and 15%, respectively) (Schroeder 1978; Dinnel et al. 1990; Kim and Park 2012). The most prominent bathymetric feature of Main Pass is a narrow (~1.9 km), deep (15 m at the thalweg) ship channel characterized by steep bathymetric gradients (Lee et al. 2013.)

In terms of discharge, Mobile Bay is the fourth largest estuary in the continental United States with an average daily freshwater input of approximately 1715 $m^3\,s^{-1}$ (Dzwonkowski et al. 2011). The Mobile River System carries the combined flows of the Alabama and Tombigbee Rivers, which account for approximately 95% of the freshwater input into Mobile Bay (Schroeder 1978). The combined average daily maximum, mean, and minimum discharge magnitudes for the Alabama River (10/1/1975 – 9/12/2012) and Tombigbee River (10/1/1960 – 9/12/2012) are 6747 $m^3\,s^{-1}$, 1715 $m^3\,s^{-1}$, and 246 $m^3\,s^{-1}$, respectively. Average daily discharge values for two distinct wet and dry seasons are 2637 $m^3\,s^{-1}$ and 802 $m^3\,s^{-1}$, respectively. Daily discharge can vary from less than 250 $m^3\,s^{-1}$ to over 15000 $m^3\,s^{-1}$

(Dinnel et al. 1990). Low flow is considered to be less than 500 m^3 s^{-1} and flood discharge to be greater than 7000 m^3 s^{-1} (Schroeder 1978; Schroeder and Lysinger 1979).

Most shallow estuaries are considered partially mixed and stratification varies greatly in response to wind and riverine discharge (Dinnel et al. 1990; Park et al. 2007; Kim and Park 2012). Multi-hour periods of strong sustained winds can mix the entire Mobile Bay vertically, except for the deeper areas, such as the navigation channel (Schroeder 1978). Riverine discharge is also important to the structure of the water column in Mobile Bay, where at any given time portions of the bay can be highly stratified while other areas will be near vertically homogenous (Schroeder 1978). During low riverine discharge rates a stratified system can exist in the upper bay (north) while the high salinity lower bay (south) waters can approach vertically homogenous (Schroeder 1978). Strong stratification of the bay has been observed for large freshwater discharges, which counteract other mixing sources, such as tides and winds (Ryan et al. 1997; Park et al. 2007). Schroeder and Wiseman (1986) report strong stratification occurs during periods of both 1) high riverine discharge and weak winds, and 2) persistent southward-directed wind stress and lower riverine discharge.

The dominant wind fields over the bay are a northwest to northeast system during the late fall and winter and a southeast to southwest system in the spring and summer (Schroeder 1978). Cold fronts associated with

convergent air masses interrupt the prevailing winds with energetic episodic

winds from the southwest and northwest (Huh et al. 1984). The

strengthening of the Bermuda high pressure system in the spring switches

the prevailing wind direction to the southeast, and by summer the winds are

weak and predominately from a southern quadrant (Dinnel et al. 1990).

Often during the summer a land-sea breeze system prevails, and during all

seasons multiple day periods of light variable winds to calms may occur

(Schroeder 1978).
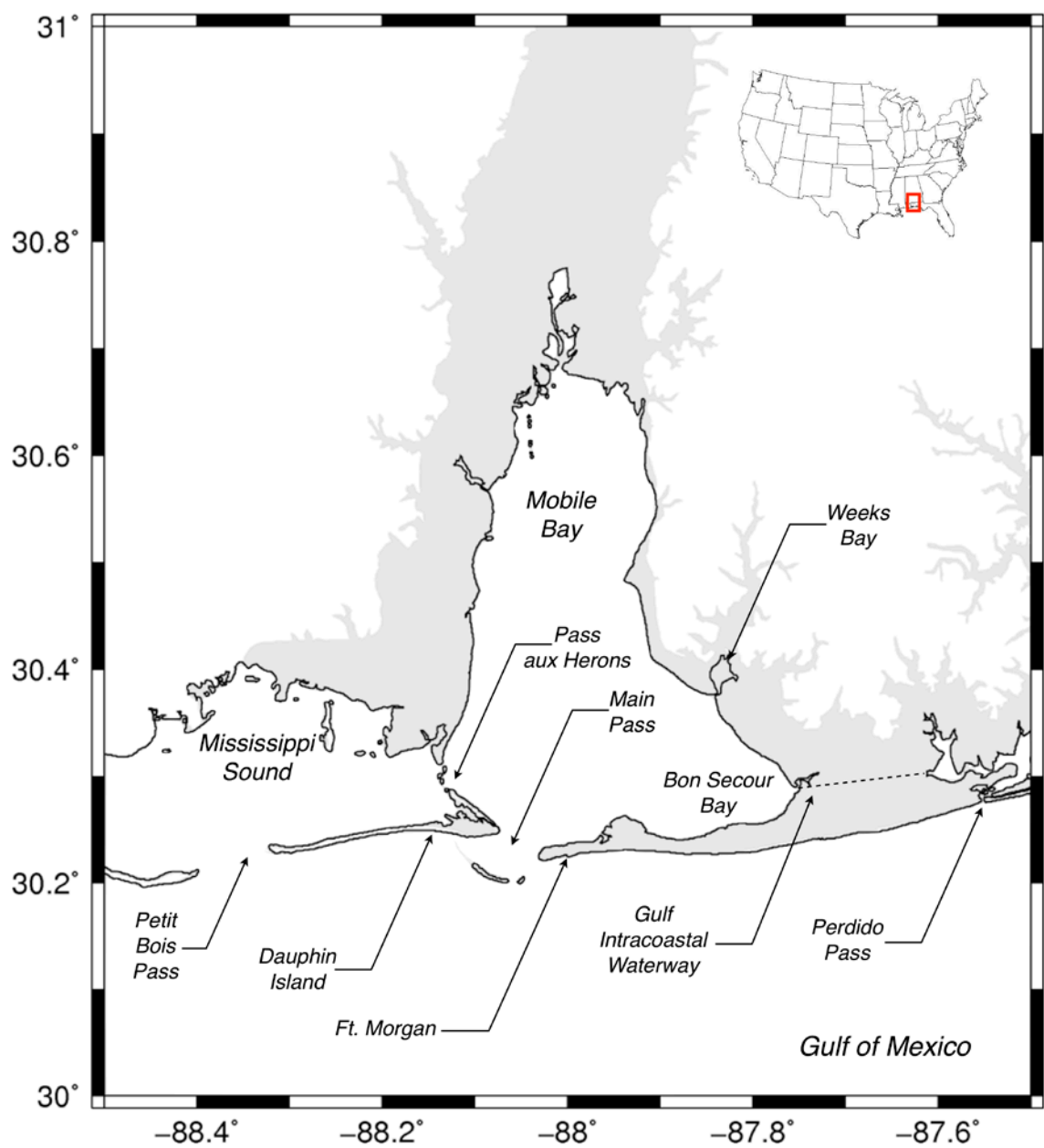
Figure 5: Points of interest within the study area, Mobile Bay, Alabama.
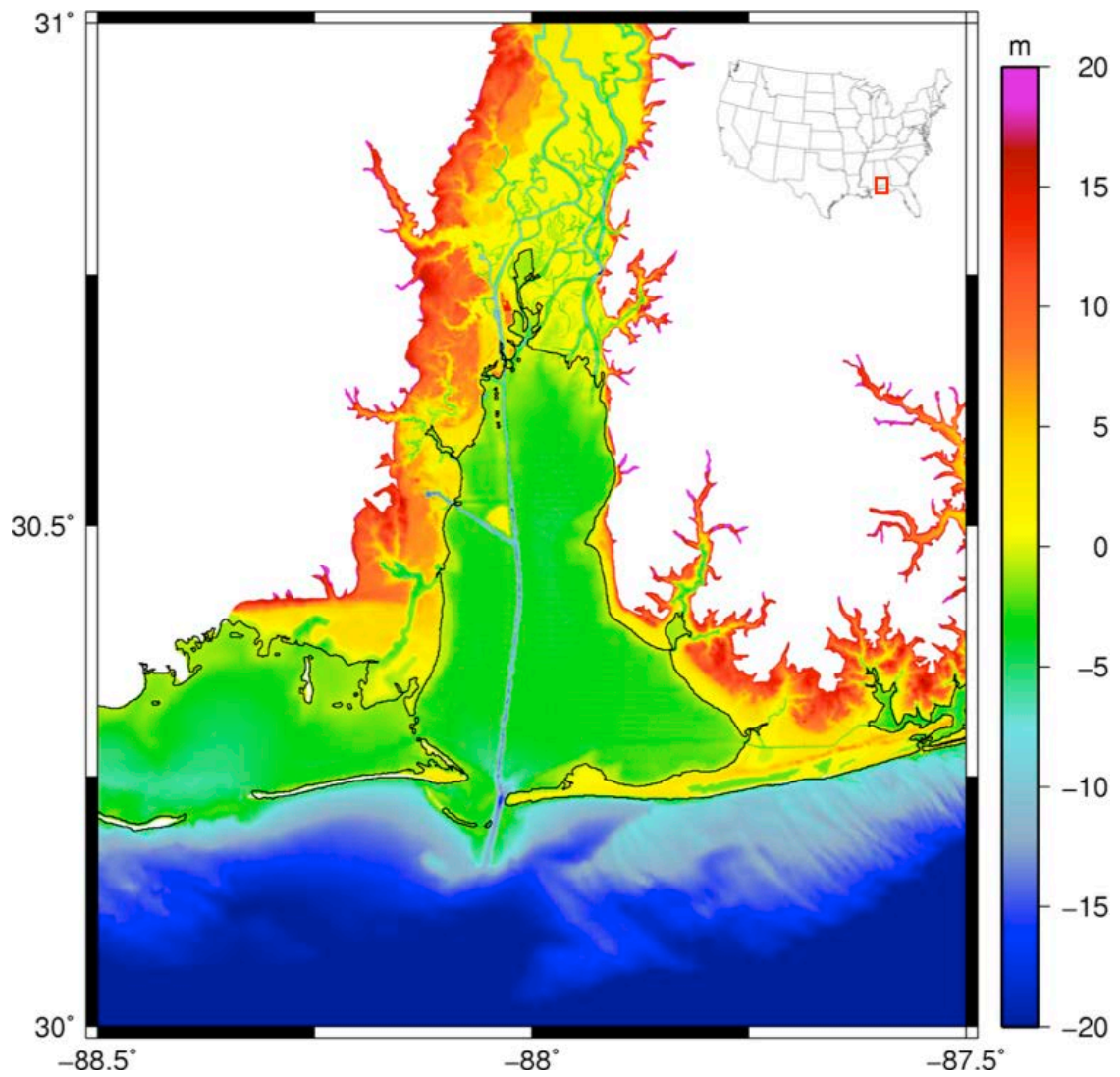
Figure 6: Shows topography and bathymetry near the study area. Elevations are relative to mean sea level.

OBJECTIVE

The primary objective of this study is to determine the spatial variability and response of hydrodynamic timescales in Mobile Bay, Alabama to riverine discharge magnitude from the Alabama and Tombigbee rivers. The residence, exposure, and flushing times for Mobile Bay, Alabama are estimated using two-dimensional hydrodynamic advanced circulation model output where tides and river flows constitute the primary forcing. A Lagrangian particle tracking model is used to track the trajectories of more than 30,000 passive tracers initialized at discrete locations throughout Mobile Bay. General hydrodynamic model parameters can be found in Table 1. These models, as well as their forcing conditions, are described in the following sections.

METHODOLOGY

Various published methodologies were used throughout this study to quantify the measurement of hydrodynamic timescales in Mobile Bay, Alabama. Historical averages of daily discharge were obtained from United States Geological Survey (USGS) recording stations (Figure 10) along the Alabama and Tombigbee rivers to identify means of daily maximum, minimum, and mean flow conditions, as well as a wet and dry season (Table 2). These data were used, along with tidal elevations, to simulate circulation patterns and water levels throughout the estuary by utilizing a sophisticated numerical model. A particle tracking model used simulated velocities to predict the trajectories of discrete particles throughout the study area. Residence time was defined as the time it took for each discrete particle to leave the study area for the first time. Exposure time was defined as the time it took for each discrete particle to leave the study area for good, and flushing time was defined as the time it took for the instantaneous concentration of the estuary to fall below $1/e$ (i.e. ~36.79%) of its initial concentration. The model's predictive capability was demonstrated through model validation with verified field observations from several tide and current velocity

recording stations. Predicted results were compared to calculations using the freshwater fraction method (Dyer 1973), a simple analytical method for quantifying flushing time.

<div align="center"><u>Hydrodynamic Model</u></div>

The Advanced Circulation (ADCIRC) model is a suite of hydrodynamic numerical models that solve time dependent, free surface circulation, and transport problems in two and three dimensions. The model utilizes unstructured meshes, and thus it allows localized refinement in regions where the solution gradients are largest (Luettich et al. 1992; Westerink et al. 1994). It is assumed that the water column is well-mixed, and therefore, vertically integrated forms of the equations are solved in the two-dimensional depth-integrated (2DDI) form of the model applied to this study. Applications of the ADCIRC-2DDI model to the English Channel and southern North Sea, the Gulf of Mexico, Masonboro Inlet, and the New York Bight have shown that it is capable of running month to year-long simulations while providing detailed intra-tidal computations (Luettich et al. 1992). General ADCIRC model parameters can be found in Table 1.

The ADCIRC model computes water levels through a solution of the Generalized Wave Continuity Equation (GWCE), which is a combined and differentiated form of the continuity and momentum equations

$$\frac{\partial^2 \zeta}{\partial t^2} + \tau_0 \frac{\partial \zeta}{\partial t} + S_p \frac{\partial \tilde{J}_\lambda}{\partial \lambda} + \frac{\partial \tilde{J}_\phi}{\partial \varphi} - S_p U H \frac{\partial \tau_0}{\partial \lambda} - V H \frac{\partial \tau_0}{\partial \varphi} = 0 \tag{1}$$

where

$$\tilde{J}_\lambda = -S_p Q_\lambda \frac{\partial U}{\partial \lambda} - Q_\varphi \frac{\partial U}{\partial \varphi} + f Q_\varphi - \frac{g}{2} S_p \frac{\partial \zeta^2}{\partial \lambda} - g S_p H \frac{\partial}{\partial \lambda}\left[\frac{P_s}{g\rho_0}\right]$$

$$+ \frac{\tau_{s\lambda,winds} + \tau_{s\lambda,waves} - \tau_{b\lambda}}{\rho_0} + (M_\lambda - D_\lambda) + U \frac{\partial \zeta}{\partial t} + \tau_0 Q_\lambda - g S_p H \frac{\partial \zeta}{\partial \lambda}$$

$$\tag{2}$$

and

$$\tilde{J}_\varphi = -S_p Q_\lambda \frac{\partial V}{\partial \lambda} - Q_\varphi \frac{\partial V}{\partial \varphi} - f Q_\varphi - \frac{g}{2}\frac{\partial \zeta^2}{\partial \lambda} - g H \frac{\partial}{\partial \varphi}\left[\frac{P_s}{g\rho_0} - \alpha\eta\right]$$

$$+ \frac{\tau_{s\varphi,winds} + \tau_{s\varphi,waves} - \tau_{b\varphi}}{\rho_0} + (M_\varphi - D_\varphi) + V \frac{\partial \zeta}{\partial t} + \tau_0 Q_\varphi - g H \frac{\partial \zeta}{\partial \varphi}$$

$$\tag{3}$$

and the vertically averaged currents are obtained from the momentum

equations

$$\frac{\partial U}{\partial t} + S_p U \frac{\partial U}{\partial \lambda} + V \frac{\partial U}{\partial \varphi} - fV = -g S_p \frac{\partial}{\partial \lambda}\left[\zeta + \frac{P_s}{g\rho_0} - \alpha\eta\right] + \frac{\tau_{s\lambda,winds} + \tau_{s\lambda,waves} - \tau_{b\lambda}}{\rho_0 H} +$$

$$\frac{(M_\lambda - D_\lambda)}{H} \tag{4}$$

$$\frac{\partial V}{\partial t} + S_p U \frac{\partial V}{\partial \lambda} + V \frac{\partial V}{\partial \varphi} + fU = -g \frac{\partial}{\partial \varphi}\left[\zeta + \frac{P_s}{g\rho_0} - \alpha\eta\right] + \frac{\tau_{s\varphi,winds} + \tau_{s\varphi,waves} - \tau_{b\varphi}}{\rho_0 H} +$$

$$\frac{(M_\varphi - D_\varphi)}{H} \tag{5}$$

where H=ζ+h is total water depth; ζ is the departure of the water surface

from the mean; h is the bathymetric depth; $S_p = \cos\varphi_0/\cos\varphi$ is a spherical

coordinate conversion factor and φ_0 is a reference latitude; U and V are the

depth-integrated currents in the λ- and φ-directions, respectively; Q_λ=UH and

Q_φ=VH are fluxes per unit width; f is the Coriolis parameter; g is the

gravitational acceleration; P_s is the atmospheric pressure at the surface; ρ_0 is

the reference density of water; η is the Newtonian equilibrium tidal potential

and α is the effective earth elasticity factor; $\tau_{s,winds}$ and $\tau_{s,waves}$ are surface

stresses due to winds and waves, respectively; τ_b is the bottom stress; M is

lateral stress gradients; D is momentum dispersion terms; and τ_0 is a

numerical parameter that optimizes the phase propagation properties (Kolar

et al. 1994; Atkinson et al. 2004).

Table 1: General ADCIRC model parameters.

Parameter	Value	Unit
Model time step	1.0	s
Ramp time	15	days
Eddy viscosity	30	m^2s^{-1}
Bottom friction	0.0025	-
Coriolis	Variable	s^{-1}
Water surface elevation offset	0.07	m
Number of Nodes	421087	-
Number of Elements	819326	-

Unstructured Mesh

The triangular, finite-element mesh used by ADCIRC in this study

contains 819,326 triangular mesh elements and 421,087 mesh nodes (Figure

7). The essential attributes of each mesh node are its horizontal positions in a

spherical coordinate system, as well as the corresponding elevation (negative

for land, positive for water) relative to a local tidal datum (i.e., mean sea

level). The horizontal positions of each node are specified as latitude and

longitude in decimal degrees relative to the North American Datum of 1983

(NAD 83). Spacing of mesh nodes (meters) ranges from O (10 km) in the Gulf

of Mexico to O (10 m) in some small tributaries. Typical mesh spacing in

Mobile Bay is O (100 m), with some exceptions (Figure 9). It should be noted

that Figure 9 also shows the spacing of Lagrangian particle tracking model

(LPTM) initial particle positions (meters) within Mobile Bay. Particles were

distributed at nodal locations within the bay and particle spacing is therefore

synonymous with mesh nodal spacing. The nodal elevations range from 2,930 m (water depth) in the North-Central Gulf of Mexico to -37 m (land surface) in a few places near the river boundaries within the Mobile Bay watershed.
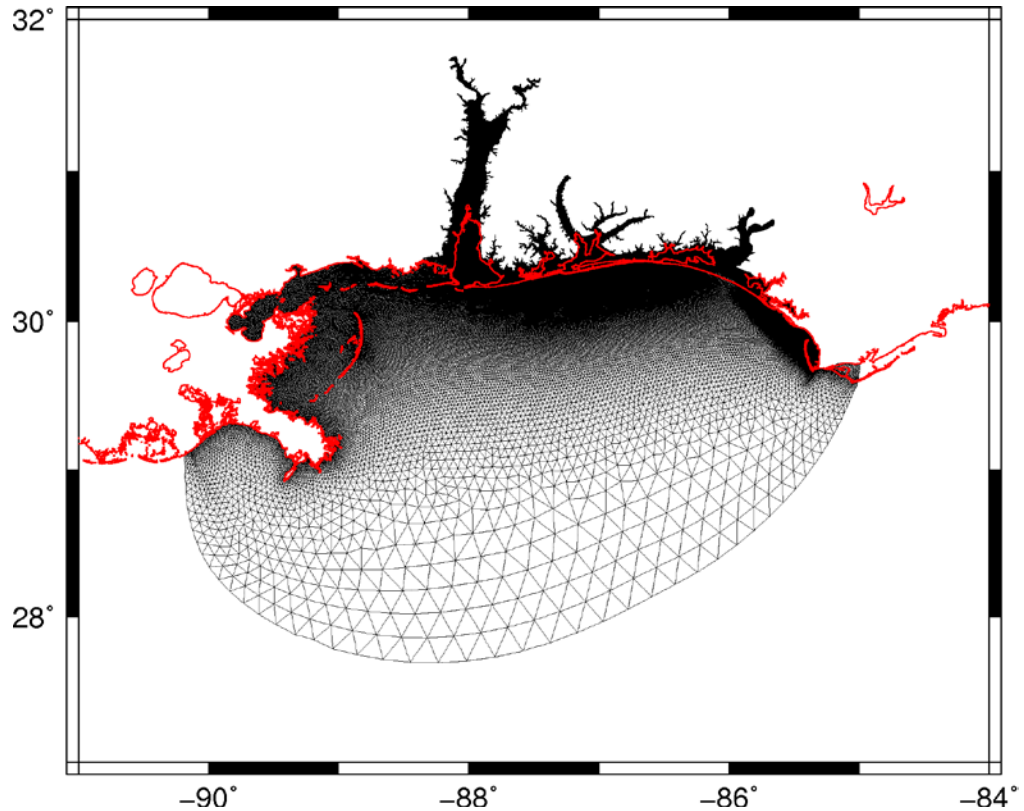
Figure 7: Distribution of triangular mesh elements for the modeling domain. The approximate shoreline location is shown in red to contrast with the mesh coverage. Note the extensive inland coverage for the watershed of Mobile Bay.

The mesh consists of 99 unique boundary segments consisting of 23,015 mesh nodes. One boundary containing 72 nodes serves as the open ocean elevation forcing boundary for tidal harmonic constituents. Two boundary

segments are used to represent the non-harmonic velocity boundary conditions of the river forcing (Figure 8). Typical mesh node spacing near inflow (river) boundaries is O (10 m). The remaining boundary segments define the landward extent of the mesh.
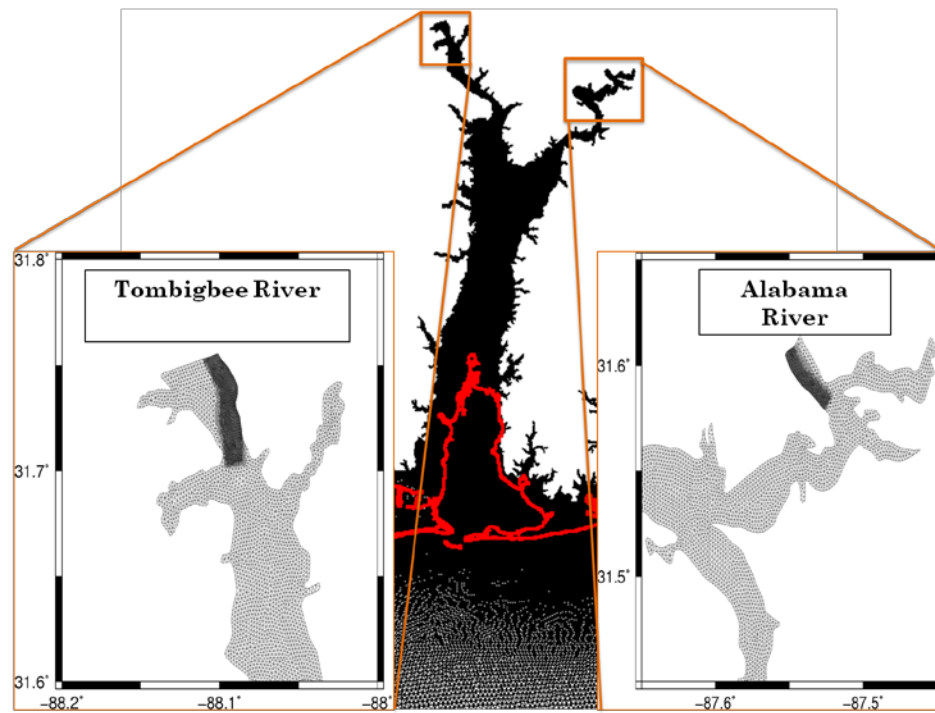
Figure 8: Local refinement of finite element mesh near river inflow boundaries. Typical mesh node spacing in refinement regions is O (10 m).

Lagrangian Particle Tracking Model

The ADCIRC model stored global velocity fields every three hours for subsequent analysis. Tracking particles were distributed at discrete locations within the mesh boundaries, or grid. The LPTM was then used to track the

transport of these discrete particles throughout Mobile Bay. Advection was assumed to be primarily forced by water current velocity, and winds where applicable. Since the primary focus of this study is to determine the effect of river discharge on residence, exposure, and flushing times, only one simulation includes meteorological forcing and is incorporated into this study as part of a comparative analysis on the impact of local meteorology on the hydrodynamic timescales. When applicable, to account for both effects, the total velocity used to advect the particles was computed as the sum of the water velocity, u_c plus a fraction of the wind velocity, u_w

$$u(x_p) = F_c u_c(x_p) + F_w u_w(x_p) \tag{6}$$

where $x_p = (x_p, y_p)$ are the scattered particle positions and F_c, F_w are multipliers for the currents and winds, respectively (Dietrich et al. 2012). In the absence of currents, F_w is often assumed to be in the range of $0.03 - 0.035$ (Reed et al. 1994).

Dispersion of particle tracers occurred with a random walk in the two horizontal dimensions. This stochastic velocity agitation was combined with the deterministic current- and wind-driven particle velocities so that

$$x_p(t + \Delta t) = x_p(t) + u(t)\Delta t + D \tag{7}$$

where $D = (D_x, D_y)$ are the horizontal diffusion agitations

$$D = (2R - 1)\sqrt{cE_v\Delta t} \tag{8}$$

and $0 \leq R \leq 1$ is a random number, $E_{v,x} = E_{v,y} = 10 m^2 s^{-1}$ are the turbulent coefficients, and $c_x = c_y = 12$ are scaling coefficients (Proctor et al. 1994).

A lattice cell search algorithm was implemented to locate the particles on the mesh. The finite-element domain was divided into lattice cell sections, and a cell-element list table was constructed. Then the particle location was searched only in elements that were contained within the same cell that contains the particle. The cell address $i=(i_x,i_y)$ was determined as follows:

$$i = int\big[(x_p - x_0)/\Delta x\big] \tag{9}$$

where $x_0=(x_0,y_0)$ are the origin of the lattice cell, and $\Delta x=(\Delta x,\Delta y)$ are the cell widths for the x- and y-coordinates. Once the finite element containing the particle was located, the velocity field was interpolated linearly to the location of the particle itself (Dietrich et al. 2012).

For this study, a total of 33,372 passive particle tracers were used in the LPTM simulations. The initial positions of these particles (Figure 9) were coincident with mesh node locations within a pre-defined study area that includes all of Mobile Bay, some of the lower Mobile-Tensaw River delta, and Dog River. The LPTM study area did not include Fowl River, the Gulf Intracoastal Waterway (GIWW), or Weeks Bay in the initialization of particle positions, but these regions were explicitly included in the ADCIRC solution and particles freely propagated into all wet mesh elements. The southern, eastern, and western boundaries for particles leaving the LPTM study area were Main Pass (latitude: 30.23ºN), the GIWW (longitude: 87.75 ºW), and Pass aux Herons (longitude: 88.132ºW), respectively (Figure 5).
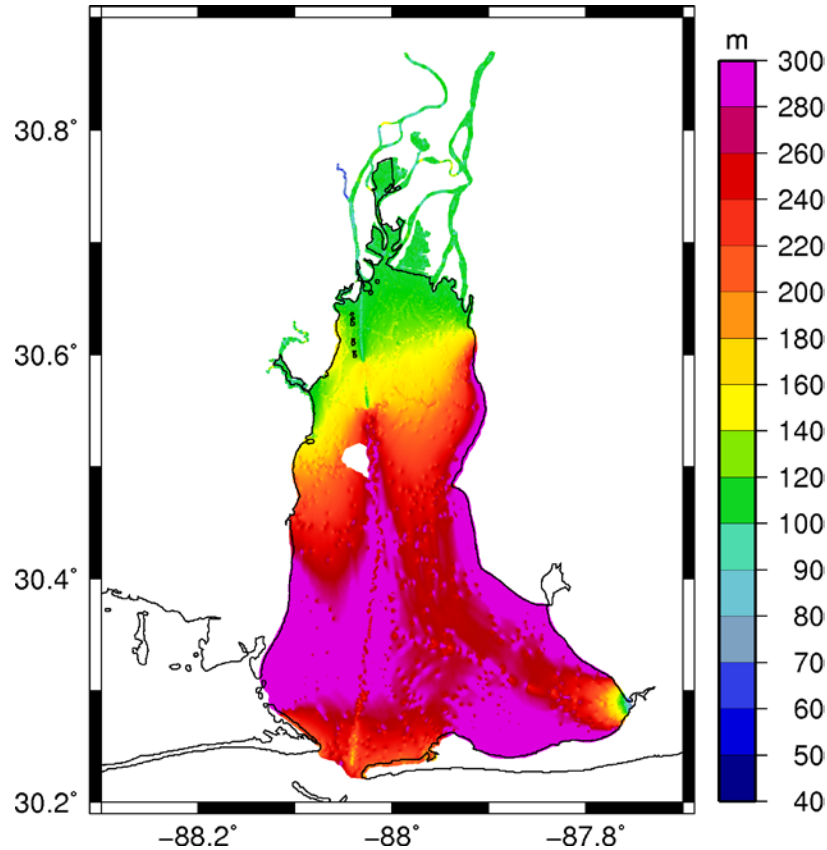
Figure 9: Spacing of particle initial positions (meters) within Mobile Bay. The nominal spacing is O (200 m). The shoreline is shown for reference only. Initial particle position coverage is indicated by the colored regions of the figure.

<u>Freshwater Fraction Method</u>

LPTM calculations of flushing time are compared to a simple box-model steady-state method (i.e. freshwater fraction method) for straightforward comparison. Simple tidal prism methods are not considered during this study, because Mobile Bay is categorized as an estuary with relatively high freshwater inflow, where salinity differences are measureable. Tidal prism methods rely on the assumption that the length of an estuary is sufficiently

short so that the estuary is horizontally and vertically homogeneous; thereby satisfying the definition of well-mixed (Luketina 1998). For many estuaries, including Mobile Bay, this assumption proves problematic, where estuarine geometry, meteorology, and riverine inflow causes variable stratification.

The easiest and most relevant criterion for choosing an appropriate method might be whether there is a salinity difference between the estuary and the ocean. Sheldon and Alber (2006) argue that in any situation where the salinities are measurably different and the freshwater fraction method can be applied, it is probably preferable. Furthermore, the freshwater fraction method has greater potential to include the combined effects of flushing from many physical processes, whereas the tidal prism model does not include gravitational circulation of seawater (Sheldon and Alber 2006).

The freshwater fraction method (Dyer 1973) estimates the flushing time (τ_{FW}) by dividing the freshwater volume of the estuary (V) by the freshwater inflow rate (Q_{FW}) averaged over a given period of time. Flushing time is then defined as,

$$\tau_{FW} = \frac{V Frac_{FW}}{Q_{FW}} \tag{10}$$

Freshwater volume is calculated by multiplying the estuary volume by the freshwater fraction, which is calculated by comparing the average estuarine salinity (S_{AVG}) to the salinity of seawater (σ) (Dyer 1973).

$$Frac_{FW} = \frac{\sigma - S_{AVG}}{\sigma} \tag{11}$$

For this study, the average estuarine salinity and salinity of seawater were assumed 30 ppt and 17 ppt, respectively.

The calculation of the freshwater fraction incorporates the seawater inflow necessary to balance the freshwater inflow and maintain the average estuarine salinity. The inference that the method does not take flushing by seawater into account is a misleading consequence of the simplification of terms in the usual presentation of the model (Sheldon and Alber 2006). A reliable estimation of flushing time can be made only if S_{AVG} is significantly different from σ. If it is not, the $Frac_{FW}$ approaches zero, which is not problematic, but $Frac_{FW}$ can be expected to covary with Q_{FW} so that the ratio in Equation 10 will be poorly constrained at very low flows (Sheldon and Alber 2006).

Numerical Experiments

A series of numerical experiments were developed to determine the spatial variability of residence time, and its response to riverine discharge magnitude without the contribution of meteorological forcing, as well as two hindcasts of observed flows and tides both including and excluding meteorology. A total of seven test cases were considered and boundary conditions can be found in Table 3. Data were obtained from the USGS Stations 2428400 and 2469761 (Figure 10) for the Alabama River and Tombigbee River, respectively. Averages of daily maximum, mean, and

minimum discharge values were obtained for the existing period of record of verified data at each site (Table 2). Discharge data periods of record for the Alabama River and Tombigbee River were October 1975 – September 2011 and October 1960 – September 2011, respectively. Note that the average observed flows are different here because of the duration of the hindcast simulations for each test case.

Wet and dry seasonality were identified based on historical discharge data for this region as December – May and June – November, respectively (Figure 11). Daily mean discharge values were averaged with respect to each season (Table 2). These values were then used as model forcing conditions for their respective simulation in ADCIRC.

Meteorological data were obtained from 20 different National Oceanographic and Atmosphere Administration (NOAA) buoys in the Northern Gulf of Mexico and Mobile Bay (Figure 12). Measurements of wind speed, direction, and pressure were interpolated to a common time-series and grid for use as meteorological forcing conditions in a 214-day hindcast simulation. Observed winds and pressures were corrected to standard reference elevations of 11 meters and sea level, respectively. These data were used for meteorological forcing in a hindcast simulation of observed flows, tides, and meteorology.
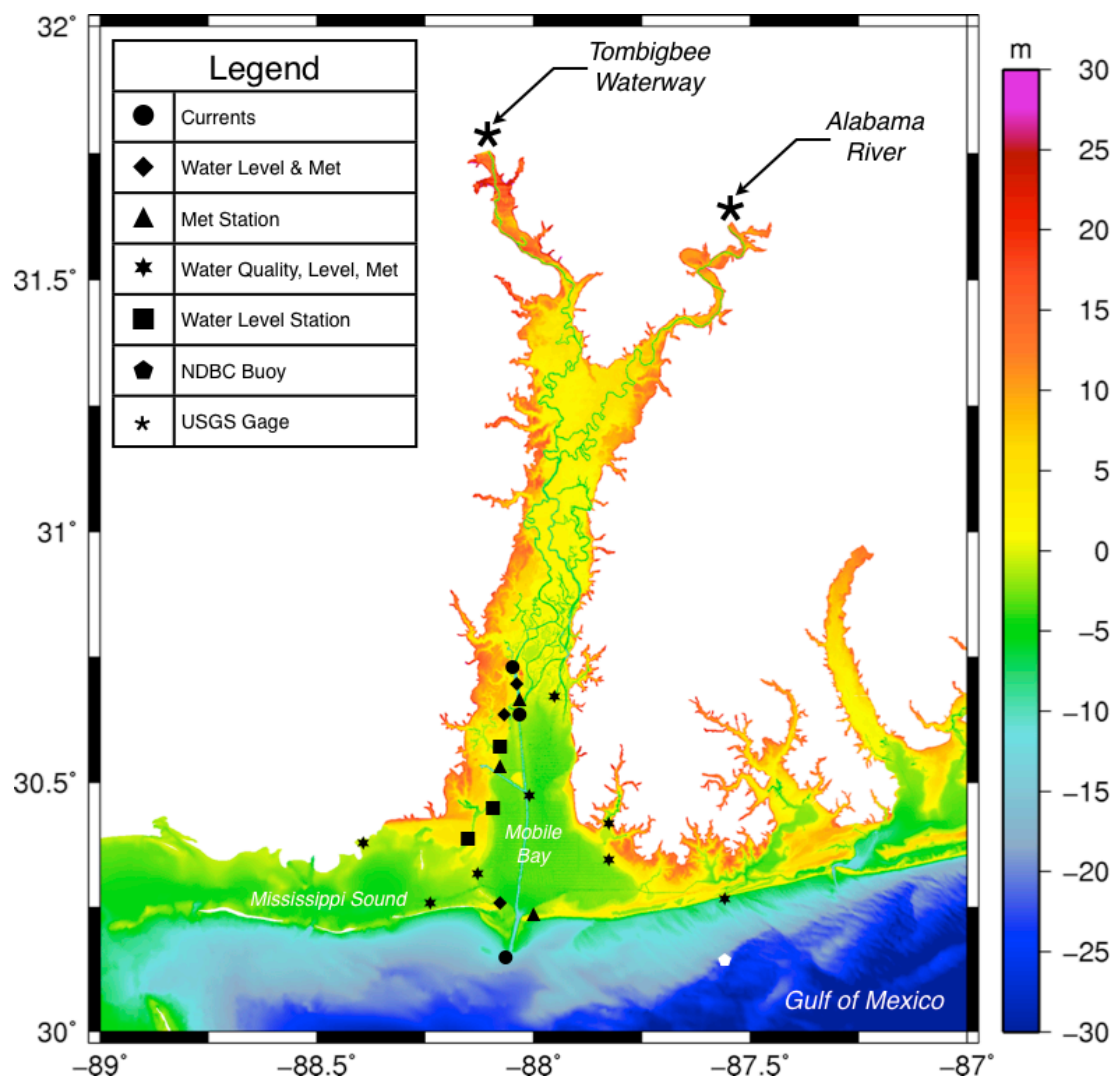
Figure 10: Bathymetry and topography within the study area with USGS gages and important data collection instrument locations identified.

Table 2: Daily average discharge values for the Alabama and Tombigbee rivers in cubic meters per second (m³s⁻¹).

Historical Yearly Discharge Averages			
Flow Condition	Alabama River (m^{3}s^{-1})	Tombigbee River (m^{3}s^{-1})	Alabama & Tombigbee (m^{3}s^{-1})
Mean of Daily Maximums	3217	3530	6747
Mean of Daily Means	878	837	1715
Mean of Daily Minimums	151	95	246
Wet Season	1289	1648	2637
Dry Season	472	330	802
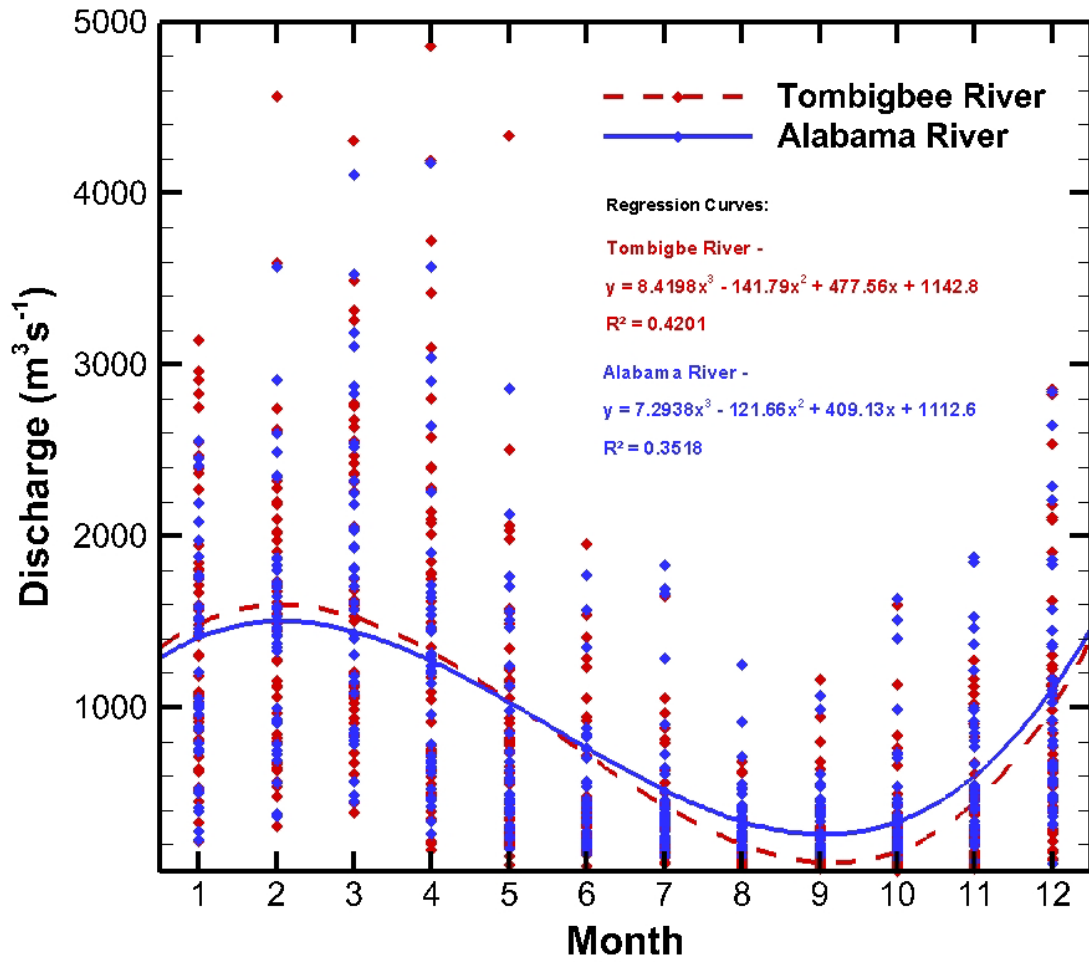
Figure 11: Monthly averages of discharge for the Alabama and Tombigbee rivers. Each symbol represents data for a respective year of record. Regression lines were fit using a 3rd order polynomial.
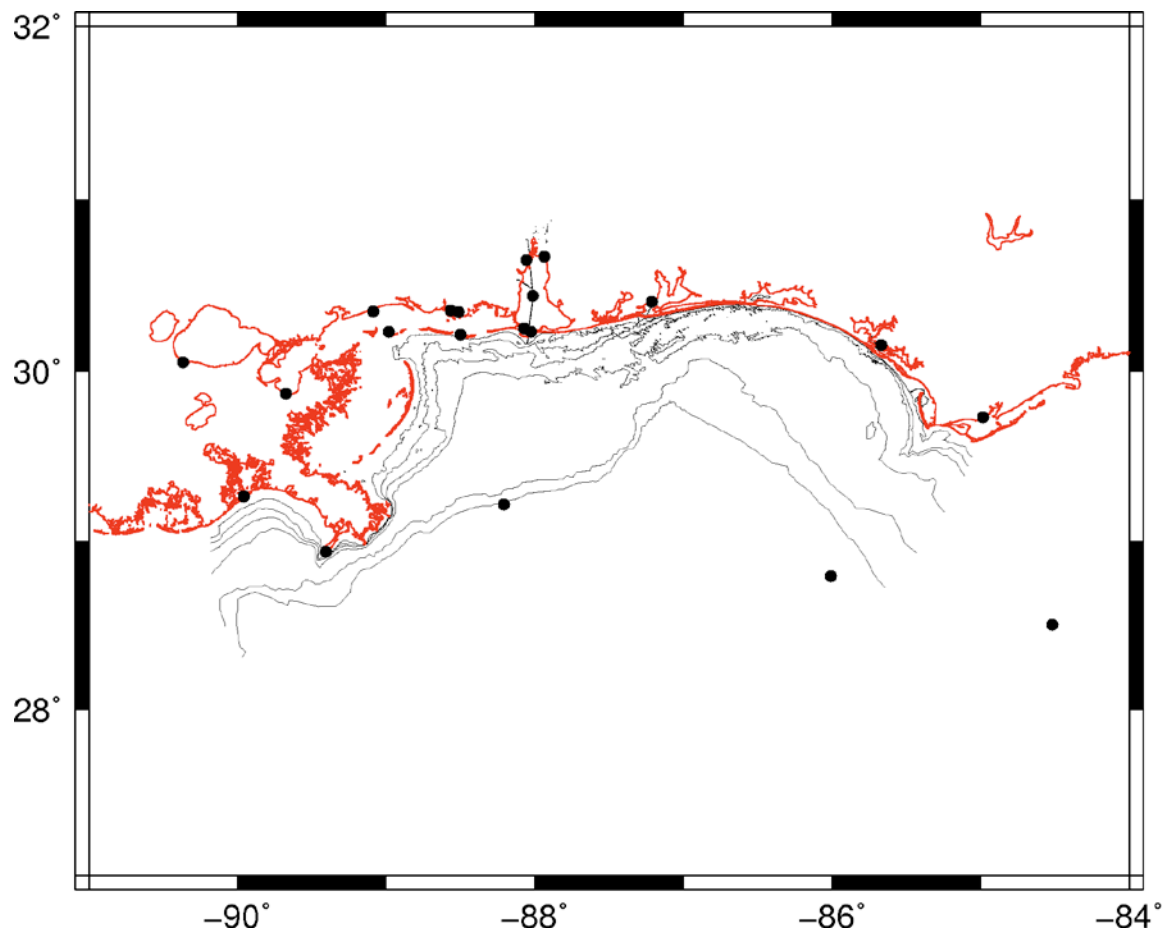
Figure 12: Locations of NOAA NBDC meteorological observation stations used to develop wind and pressure fields for the 214-day hindcast simulation of tides, observed flows and meteorological forcing. Each of the twenty (20) black dots represents an individual NDBC buoy or shore-based station.

Table 3: Critical boundary conditions for each numerical experiment

Simulation Boundary Conditions			
Test Case	Discharge (m^3s^{-1})	Tidal Constituents	Meteorlogical Forcing
1.) Maximum	6747^x	K_1, O_1, P_1, Q_1, K_2, L_2, M_2, N_2, S_2, T_2	No
2.) Mean	1715^x	K_1, O_1, P_1, Q_1, K_2, L_2, M_2, N_2, S_2, T_2	No
3.) Minimum	246^x	K_1, O_1, P_1, Q_1, K_2, L_2, M_2, N_2, S_2, T_2	No
4.) Wet Season	2637^x	K_1, O_1, P_1, Q_1, K_2, L_2, M_2, N_2, S_2, T_2	No
5.) Dry Season	802^x	K_1, O_1, P_1, Q_1, K_2, L_2, M_2, N_2, S_2, T_2	No
6.) Observed Flows (Full Meteorology)	637 *	K_1, O_1, P_1, Q_1, K_2, L_2, M_2, N_2, S_2, T_2	Yes
7.) Observed Flows (No Meteorology)	411 *	K_1, O_1, P_1, Q_1, K_2, L_2, M_2, N_2, S_2, T_2	No
[x] Steady Flows			
*Average of Variable Observed Flows			

RESULTS

Results from model validation and LPTM simulations are presented in the following sections. Based on hydrodynamic model simulations of temporal and spatial particle distributions, residence, flushing, and exposure times were calculated and averaged over the entire study area. The results are averaged over the first 24-hours to remove the initial dependence on tidal phase from the results. Each test case's results were analyzed using visual representations of exposure and residence time spatial variability; spatial averages of residence, flushing, and exposure times; and routine statistical analysis.

Model Validation

Model validation was achieved by comparing ADCIRC hindcast simulation output (Test Case 6) to verified water surface elevation and velocity data at various recording stations throughout the study area (Figure 13 and Figure 14, respectively). ADCIRC hindcast model results (including meteorology) were compared to surface elevation data obtained from NOAA CO-OPS, Mobile Bay NEP / DISL, and Weeks Bay NERRS at seven tide

stations (Figure 13) including Bon Secour Bay (BSB), Cedar Point (CPT), Dauphin Island (DI), Meaher State Park (MSP), Middle Bay Lighthouse (MBL), Mobile State Docks (MSD), and Weeks Bay (WB) (Figure 15(a)-(f)). Water level data obtained from tide stations were demeaned for comparison, as no consistent vertical datum was available for all measurements. ADCIRC water levels were interpolated from hourly observations to match the measurement frequency of the corresponding tide station. Acoustic Doppler Current Profiler (ADCP) water current velocity data obtained from NOAA PORTS were compared to model output at three locations (Figure 14) including Mobile Bay Buoy M (MB0101), Mobile Container Terminal (MB0401), and Mobile State Docks Pier E (MB0301) (Figure 16, Figure 17, & Figure 18, respectively). ADCIRC velocity data were interpolated from one-hour observations to six-minute observations to match ADCP data. The model-data comparison generally covered the period June 16, 2011 – July 15, 2011 (i.e. model days $15 - 45$). As a quantitative assessment for the model-data comparison the root-mean-square error (RMSE) was calculated for each location, which was defined as:

$$RMSE = \sqrt{\frac{\sum_{i=1}^{N}(\eta_i - \widehat{\eta_i})^2}{N}} \tag{12}$$

where N was the number of observations, η was measured data and $\widehat{\eta_i}$ was predicted.
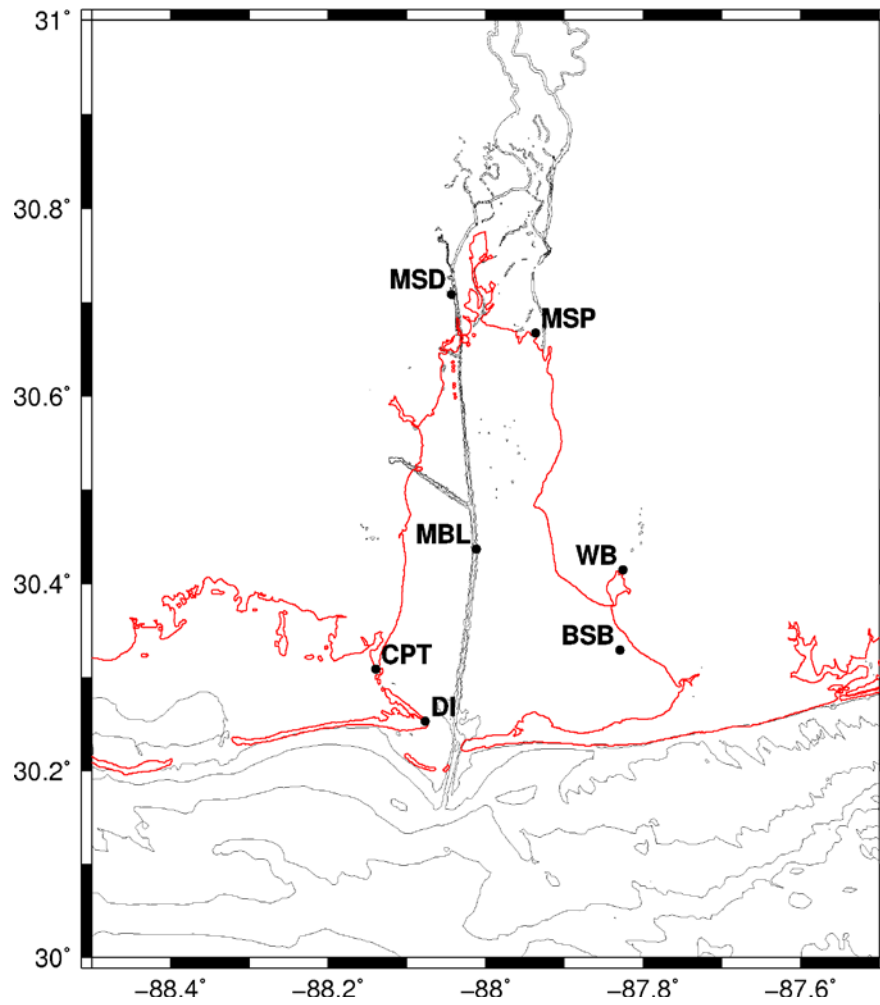
Figure 13: Water surface elevation recording sites used for model validation throughout study area. Bathymetric contours are shown using intervals of 5 meters.
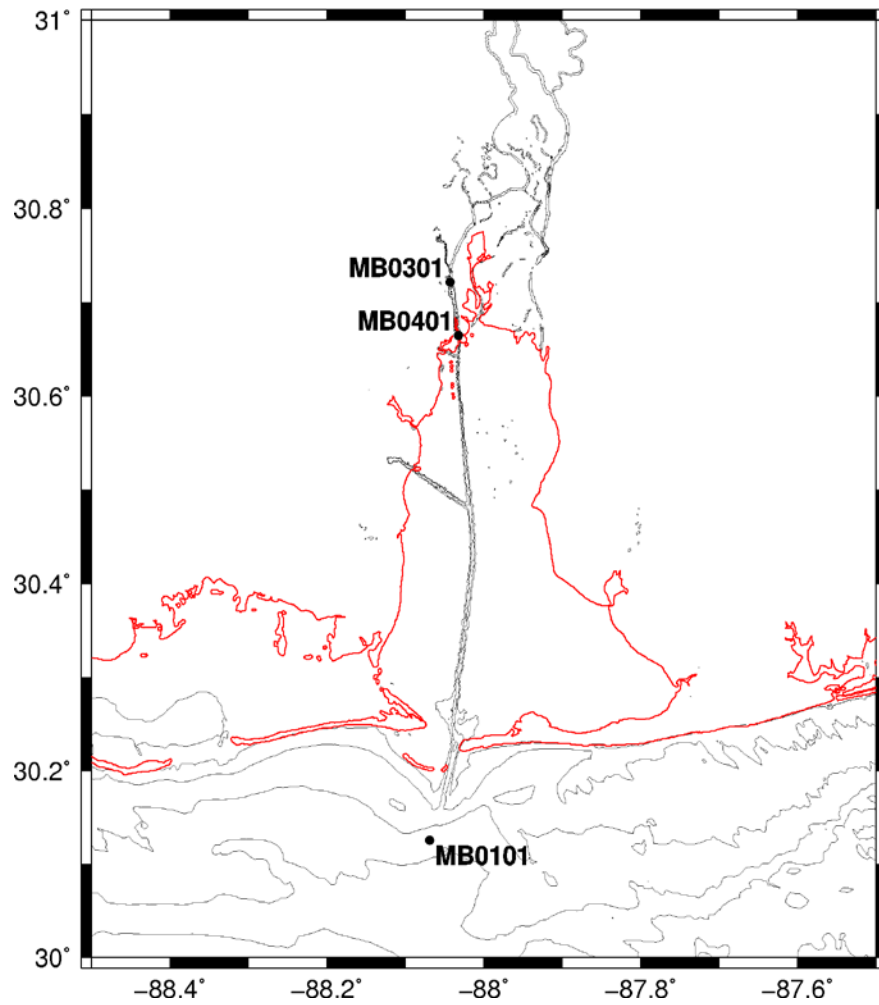
Figure 14: ADCP velocity recording sites used for model validation throughout study area. Bathymetric contours are shown using intervals of 5 meters.

Water surface elevation model output compared well to observed data throughout the study area (Figure 15 (a)-(f)). It should be noted that to obtain model stability during high flow condition test cases (e.g. maximum and wet season), it was necessary to set the model parameter eddy viscosity at 30 m^2 s^{-1}. All seven test case simulations were run under the same model parameters for consistency. While this assumption was an over estimate for low flow condition test cases (e.g. dry, mean, and minimum), model validation results showed it did not unreasonably bias results as each location's RMSE was equal to or less than 0.1 m (Figure 15 (a)-(f)). In fact, when comparing preliminary testing water level output, the RMSE of simulations with eddy viscosity equal to 30 m^2 s^{-1} were better (i.e. RMSE was smaller) at DI and only slightly worse at MSD (i.e. RMSE was greater) than simulations with eddy viscosity equal to 10 m^2 s^{-1}. A single factor ANOVA was performed to ensure model predicted water levels were statistically similar to observed water levels. The results from each case showed there was no statistical difference at a 95% confidence interval for model predicted and observed water levels based on $p > 0.05$ and $F \ll F_{critical}$. Recorded data from observation site MBL were not complete and contained no consistent sampling frequency, and therefore were not used during analysis.
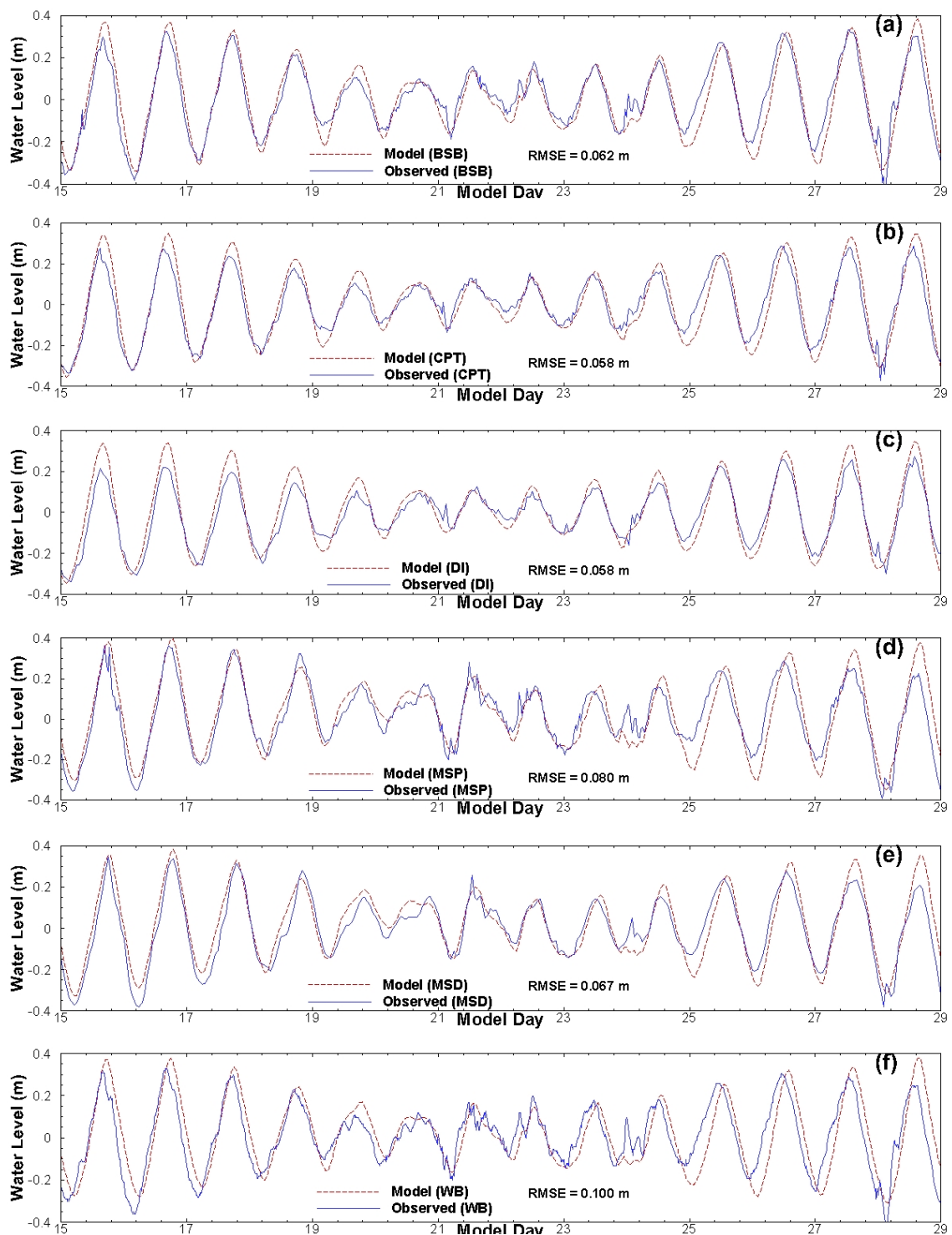
Figure 15: A comparison of model predicted and observed water levels at (a) Bon Secour Bay, (b) Cedar Point, (c) Dauphin Island, (d) Meaher State Park, (e) Mobile State Docks, (f) Weeks Bay.

43

Velocity observations were compared to ADCIRC model output at three discrete locations (Figure 16, Figure 17, and Figure 18). Current velocity directions were consistent with ADCIRC definition where u and v velocity components are increasingly positive to the east and north, respectively. In general, model output predicted u velocity components better (i.e. RMSE were smaller) than v velcoity components at the Mobile Container Terminal and Moblie State Docks, and worse (i.e. RMSE were greater) for Mobile Bay Buoy M. For example, the RMSE at the Mobile Container Terminal and State Docks was approximately one-quarter of the RMSE for the u velocity component at Mobile Buoy M (Figure 16, Figure 17, and Figure 18). However, the RMSE for the v velocity component at Mobile Buoy M was slightly more than one-half the RMSE at Mobile Containter Terminal and State Docks (Figure 16, Figure 17, & Figure 18). A single factor ANOVA was performed to ensure model predicted currents were statistically similar to observed water currents at three sampling sites in Mobile Bay. The results from each locations showed there was no statistical difference at a 90% confidence interval for model predicted and observed water currents based on $p > 0.05$ and $F \ll F_{critical}$, except for the V velocity component at the Mobile Container Terminal (MB0401) sampling site. It should be noted there are inherent difficulties associated with comparing model predicted velocity output to ADCP measurements since the ADCP measurements are from a fixed position in the water column and model output is a depth averaged value.

Mobile Bay Buoy M (MB0101) was a downward looking Nortek ADP deployed in 17.7 meters of water (latitude: 30.1253 ºN; longitude: 88.0687 ºW). The sensor was deployed 3.2 meters below the surface and had a vertical bin size of 1.0 m. A total of 13 vertical bins were measured with the first bin at 4.3 m below the surface and the last bin at 16.3 m below the surface. The MB0101 velocity measurements were averaged over depth for direct comparison to the depth integrated ADCIRC velocity output at the buoy coordinates.

Mobile Containter Terminal (MB0401) was a sideward looking Sontek ADP deployed in 13.7 meters of water (latitude: 30.6644 ºN; longitude: 88.0322 ºW) and profiled velocity measurements across the waterbody at the sensor depth (5.2 m). The sensor was deployed 5.2 meters below the surface and had a bin size of 4.0 m. Mobile Container Terminal velocity measurements from the first three bins closest to the sensor head were averaged for comparison to ADCIRC output.

Mobile State Docks Pier E (MB0301) was a sideward looking Sontek ADP deployed in 12.0 meters of water (latitude: 30.7211 ºN; longitude: 88.0428 ºW) and profiled velocity measurements across the waterbody at the sensor depth (5.3 m). The sensor was deployed 5.3 meters below the surface and had a bin size of 4.0 m. Mobile State Docks Pier E velocity measurements from the first three bins closest to the sensor head were averaged for comparison to ADCIRC output.
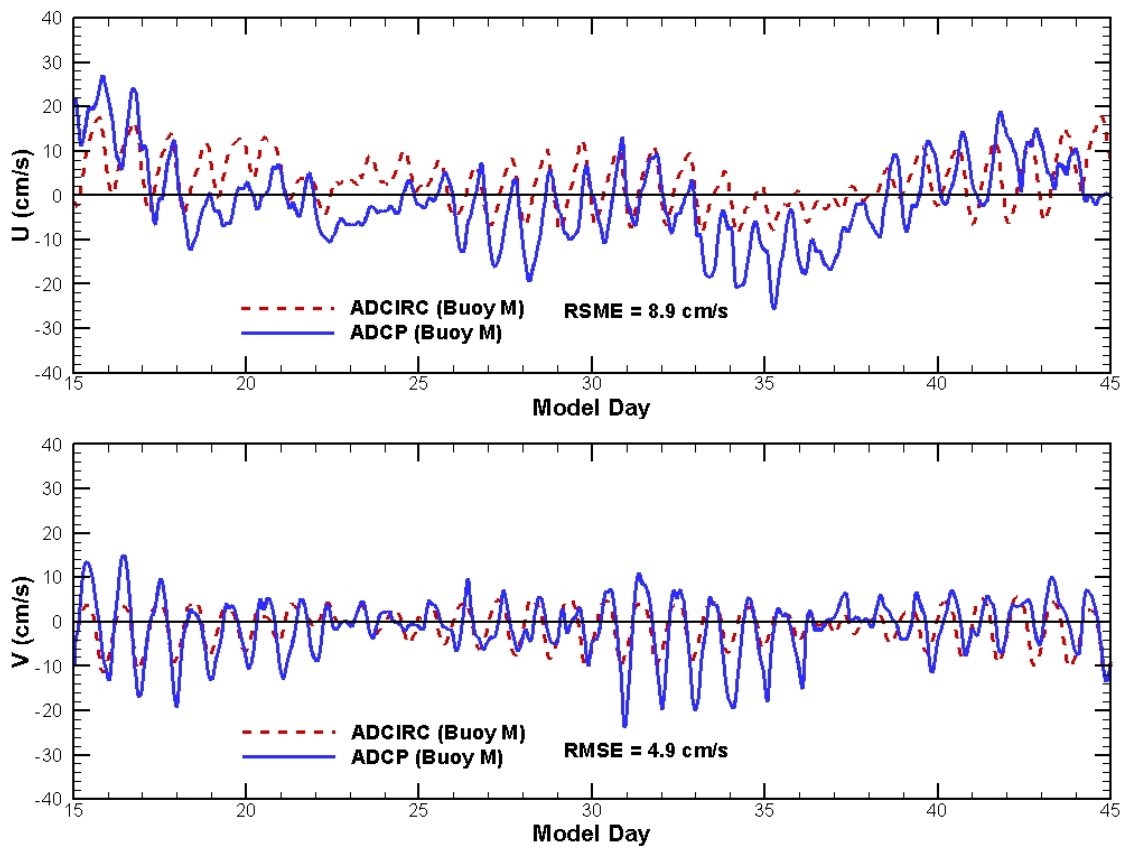
Figure 16: A comparison of measured (___) and predicted (- - -) currents at MB0101 Mobile Bay Buoy M.
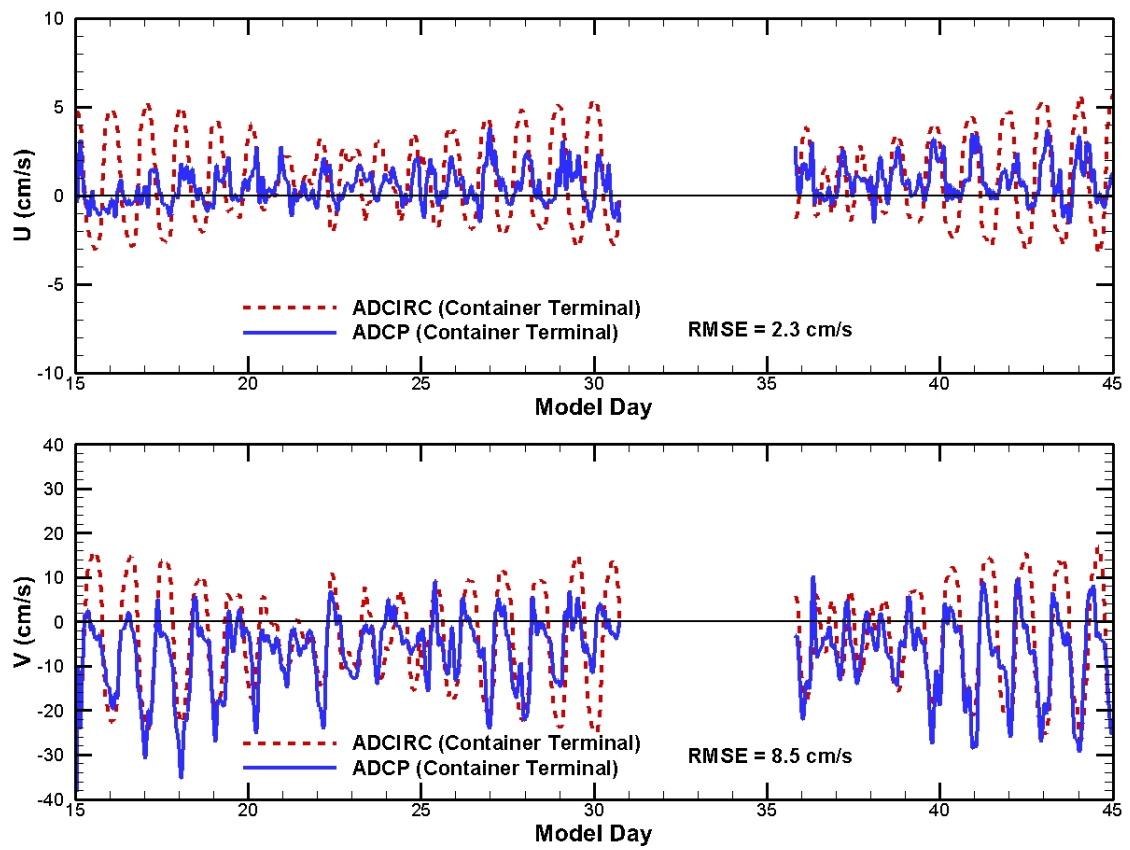
Figure 17: A comparison of measured (__) and predicted (- - -) currents at Mobile Container Terminal.
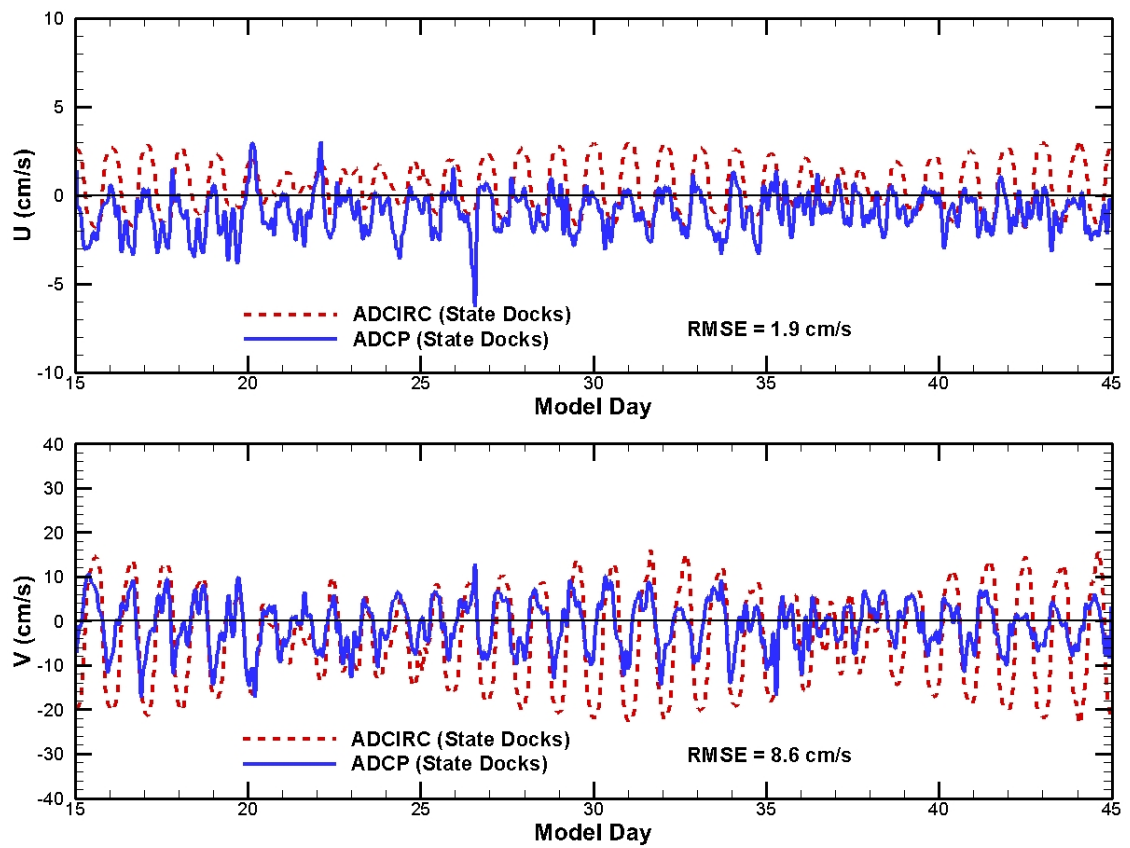
Figure 18: A comparison of measured (__) and predicted (- - -) currents at Mobile State Docks.

Exposure and Residence Timescales: Spatial Variability

Spatial variability of exposure and residence timescales in Mobile Bay was analyzed by plotting LPTM results by their spherical coordinates. LPTM data were triangulated within the study area boundaries, and contoured at 14-day intervals. The spatial variability of exposure and residence timescales, as a function of particle initial position, were generated (Figure 19 – Figure 25), and interpreted as the amount of time required for a particle starting at a specific location in the study takes to leave the study area. Residence time was defined as the amount of time for a particle to leave the system for the first time, and exposure time was defined as the amount of time for a particle to leave the system for good. It should be noted that timescales longer than 140 days were observed for Test Cases 3 and 6, but for consistency and visual representation purposes identical legends and contour intervals were utilized.

In general, exposure and residence times exhibit similar behavior for each test case; however, by definition, any discrete particle's exposure time should always be greater than or equal to its residence time. Spatial variability differed for each case, but in most cases, longer timescales were observed along the eastern and northern sections of the bay than were observed along the western and southern sections (Figure 19 – Figure 25). This trend became less apparent as the discharge increased, and the bay became more homogeneous in terms of the observed timescales. For all flow conditions, the

longest exposure and residence times were observed along the Bay's eastern shoreline, in the mid-section of Bon Secour Bay, and in the Mobile-Tensaw Delta. However, shorter timescales were observed for all flow conditions in the most southeastern section of Bon Secour Bay (Figure 19 - Figure 25), near the Gulf Intracoastal Waterway (GIWW).

Under maximum flow conditions, residence and exposure timescales varied with respect to a particle's initial spatial position, ranging from less than 3 days to approximately 75 days (Figure 19). Timescales less than 14 days were observed across a large portion of Mobile Bay, and at this contour interval the bay appeared to respond somewhat homogenously. Sections of the bay near Main Pass, Pass aux Herons, and GIWW showed the shortest timescales, while the longest timescales were observed along the eastern shoreline of Mobile Bay and the mid-section of Bon Secour Bay.
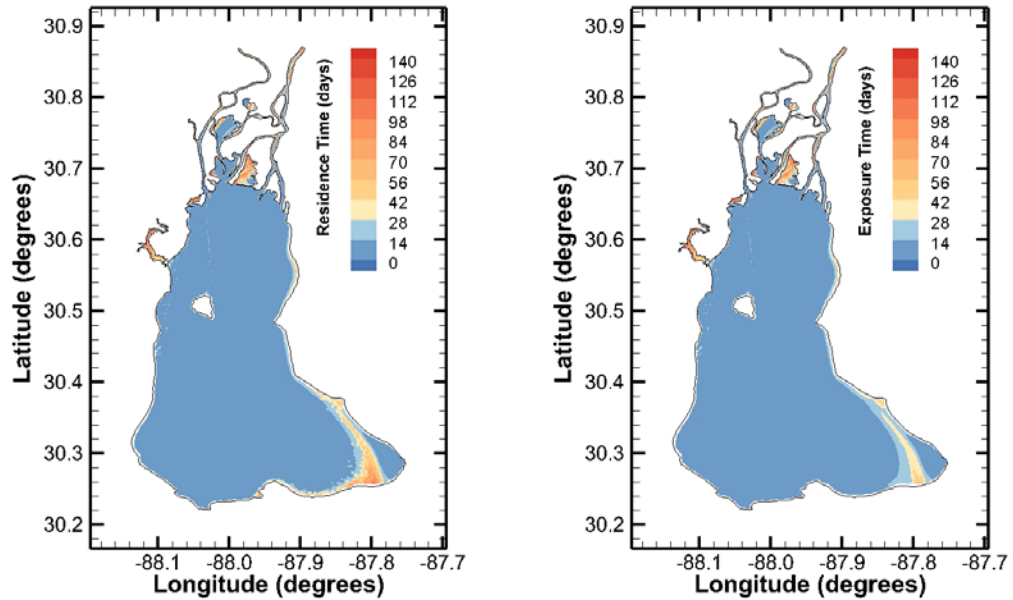
Figure 19: Spatial variability of residence and exposure times for the mean of the daily maximum flows (Test Case 1). Maximum steady flow conditions were 6747 m³ s⁻¹.

Under mean flow conditions, residence and exposure timescales varied with respect to a particle's initial spatial position, ranging from less than 14 days to approximately 100 days (Figure 20). Similar contour patterns were observed to that of maximum flow conditions (Figure 19); however, more spatial variation of contour lines was observed, especially throughout Bon Secour Bay. Sections of the bay near Main Pass, Pass aux Herons, and GIWW showed the shortest timescales, while the longest timescales were observed along the eastern shoreline of Mobile Bay and the mid-section of Bon Secour Bay.

51
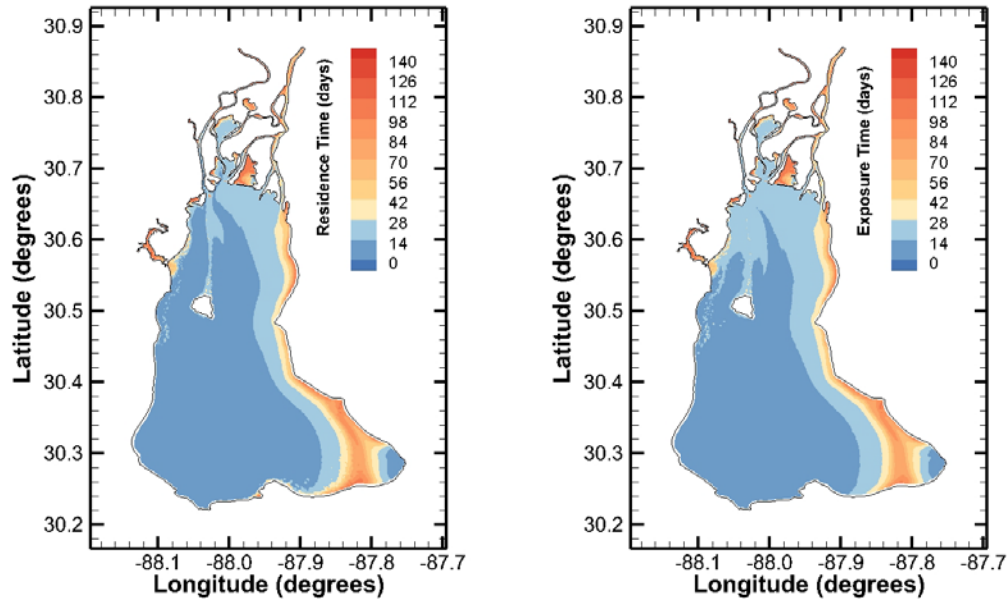
Figure 20: Spatial variability of residence and exposure times for the mean of the daily mean flows (Test Case 2). Mean steady flow conditions were 1715 m³ s⁻¹.

Under minimum flow conditions, residence and exposure timescales varied greatly with respect to a particle's initial spatial position, ranging from less than 14 days to approximately 160 days (Figure 21). Sections of the bay near Main Pass, Pass aux Herons, and GIWW showed the shortest timescales, while the longest timescales were observed along the eastern shoreline of Mobile Bay and the mid-section of Bon Secour Bay. It should be noted that the minimum flow test case was extended from 120 to 160 days in order to reveal the flushing time.
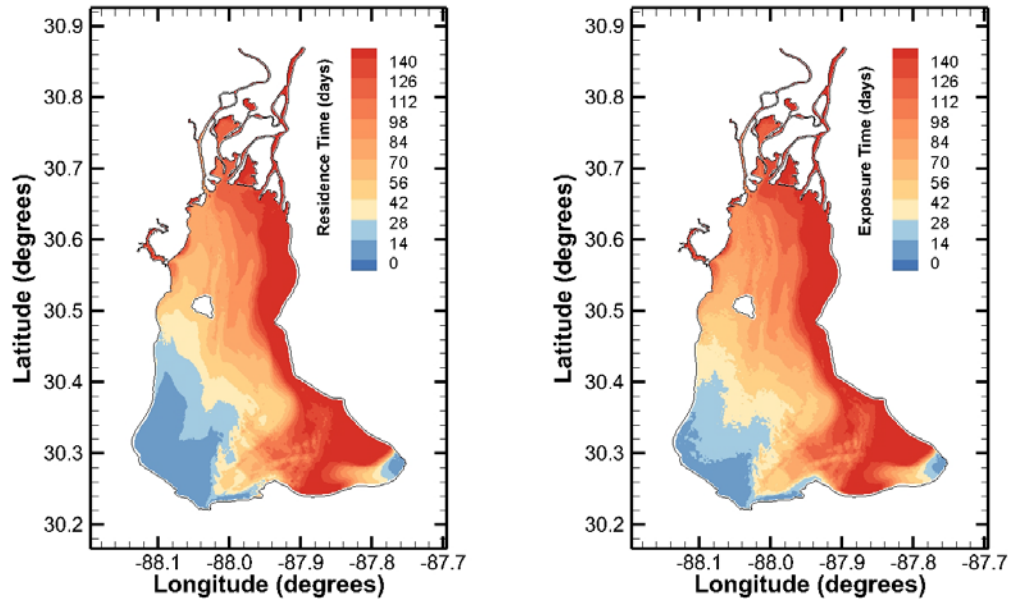
Figure 21: Spatial variability of residence and exposure times for the mean of daily minimum flows (Test Case 3). Minimum steady flow conditions were 246 m³ s⁻¹.

Under wet season flow conditions, spatial distributions of exposure and residence times varied with respect to initial particle position (Figure 22). In general, exposure and residence times less than 14 days were observed throughout the majority of the Mobile Bay for wet season conditions. Model predicted timescales ranged from less than 3 days near Mass Pass and Pass aux Herons to approximately 100 days near eastern section of Bon Secour Bay. The northern section of the bay showed timescales of approximately 50 days.
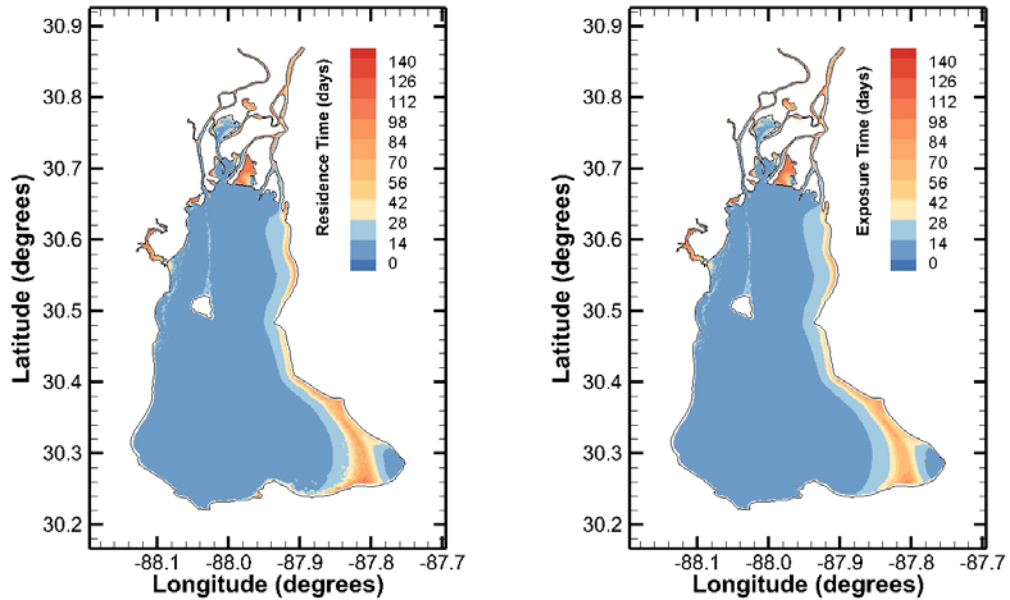
Figure 22: Spatial variability of residence and exposure times for the mean of the average daily flows during the wet season, December - May (Test Case 4). Wet season steady flow conditions were 2637 m³ s⁻¹.

Under dry season flow conditions, exposure and residence time spatial distributions were more variable than for wet season flow conditions. Model simulated timescales ranged from less than 14 days in small sections near Main Pass and Pass aux Herons to approximately 100 days near the eastern sections of Bon Secour Bay (Figure 23). The northern section of the bay showed timescales of approximately 50 days. Longer timescales also become visible adjacent to the shipping channel north of Galliard Island.
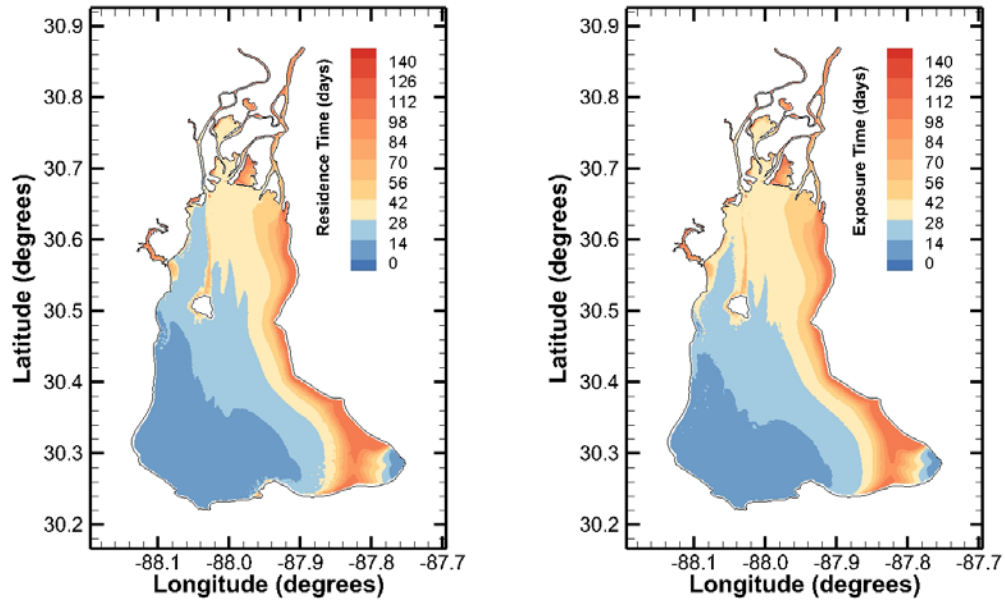
Figure 23: Spatial variability of residence and exposure times for the mean of the average daily flows during the dry season, June – November (Test Case 4). Dry season steady flow conditions were 802 m^3 s^{-1}.

Residence and exposure timescales varied with respect to a particle's initial spatial position, ranging from less than 3 days to greater than 200 days based on LPTM output for the 214-day hindcast simulation of predicted tides, observed flows, and measured meteorology. In general, the shortest timescales were observed in sections of the bay near Main Pass and Pass aux Herons, and the longest timescales were observed along the eastern shoreline of Mobile Bay, in the Mobile-Tensaw Delta, and in Bon Secour Bay (Figure 24). Shorter timescales comparable to other test cases were not observed near the GIWW for Test Case 6. It should be noted that although timescales greater than 140 days were observed during Test Case 6 for consistency

purposes the same legend and contour intervals are shown in Figure 24 and Figure 25.
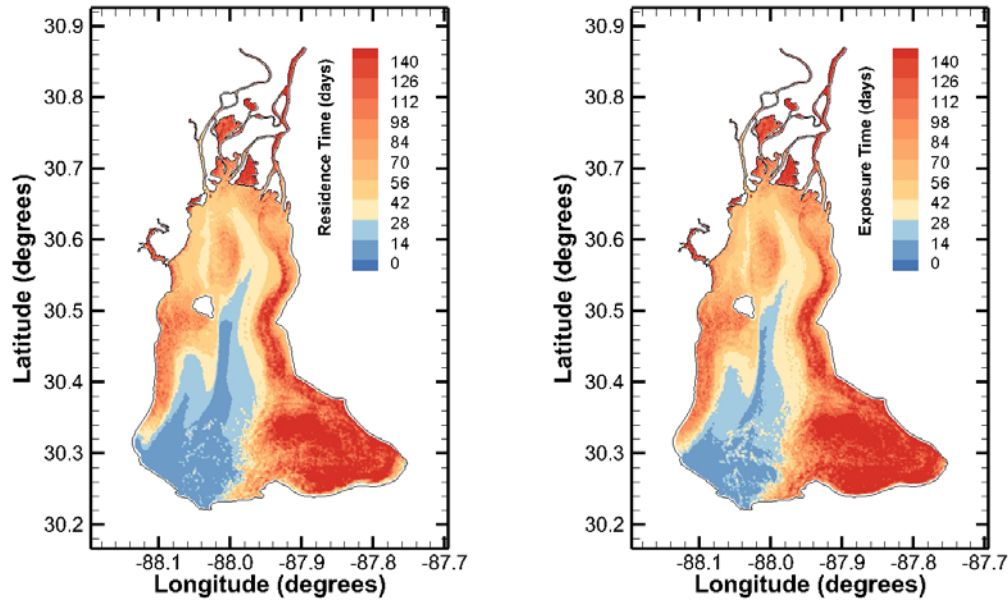
Figure 24: Spatial variability of residence and exposure times for the 214-day (June 1, 2011 – December 31, 2011) hindcast simulation of tides, observed flows, and meteorological forcing (Test Case 6). The average of the observed daily flows was 637 m³ s⁻¹.

Residence and exposure timescales varied with respect to a particle's initial spatial position, ranging from less than 3 days to greater than 140 days based on LPTM output for the 160-day hindcast simulation of tides and observed flows only (Figure 25). In general, the shortest timescales were observed in sections of the bay near the GIWW, Main Pass, and Pass aux Herons, and the longest timescales were observed along the eastern shoreline of Mobile Bay, in the Mobile-Tensaw Delta, and in Bon Secour Bay. Longer

56

timescales also become visible adjacent to the shipping channel north of Galliard Island.
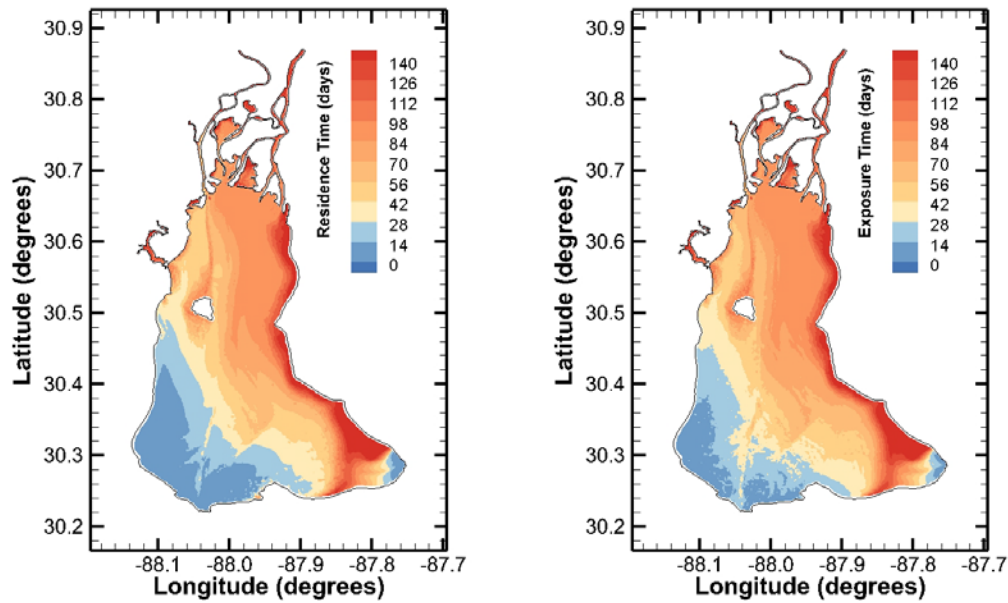
Figure 25: Spatial variability of residence and exposure times for the 160-day (June 1, 2011 – November 7, 2011) hindcast simulation of tides and variable observed flows (Test Case 7). The average of the observed daily flows was 411 m³ s⁻¹.

Flushing Times and Spatially Averaged Exposure & Residence Times

LPTM model output was spatially averaged across the study area to yield a single estimate of exposure and residence time; flushing times were determined when the instantaneous concentration of particles in the study area falls below 1/e (Table 4). The equations used to determine spatially averaged residence and exposure timescales and flushing times were given by Eqs. (13), (14), and (15), respectively.

57

$$\bar{T}_r = \frac{1}{N}\Sigma_{i=1}^{N}\,T_{r_i} \tag{13}$$

$$\overline{T}_e = \frac{1}{N}\Sigma_{i=1}^{N}\,T_{e_i} \tag{14}$$

$$C(T_f) \leq 1/e \tag{15}$$

where N is the number of particles, T_r is the residence time, T_e is the exposure time, and T_f is the flushing time, and $C(T_f)$ is the concentration of particles remaining in the study area at time T_f. The subscript i denotes the timescale value of the ith particle, and the overbar denotes an average value.

The spatially averaged exposure and residence times in Mobile Bay showed an inverse relationship to the magnitude of steady, riverine discharge. For example, as steady flow conditions increased from minimum to maximum magnitudes of steady, riverine discharge (i.e. 246 $m^3\,s^{-1}$ to 6747 m^3 s^{-1}), the average exposure and residence times decreased by 89.7 and 73.5 days, respectively (Table 4). The same relationship was observed for flushing time and increases in steady, riverine discharge. For example, as steady flow conditions increased from minimum to maximum magnitudes of steady, riverine discharge (i.e. 246 $m^3\,s^{-1}$ to 6747 $m^3\,s^{-1}$), the flushing time decreased by 127.9 days. No exceptions were observed.

Table 4: Summarizes Mobile Bay, Alabama LPTM simulation results of spatially averaged residence and exposure times, as well as flushing times in days for each test case

Test Case	Discharge ($m^3 s^{-1}$)	Mean Residence Time and Standard Deviation (days)			Mean Exposure Time and Standard Deviation (days)			Flushing Time (days)
1.) Maximum	6747 [x]	8.3	±	16.5	10.6	±	22.1	3.8
2.) Mean	1715 [x]	19.8	±	20.3	25.4	±	27.4	17.2
3.) Minimum	246 [x]	81.8	±	41.3	100.3	±	41.6	130.7
4.) Wet Season	2637 [x]	15.0	±	18.9	19.9	±	26.8	11.2
5.) Dry Season	802 [x]	35.1	±	22.8	41.8	±	27.4	40.2
6.) Observed Flows (Full Meteorology)	637 *	76.0	±	46.9	83.4	±	48.5	82.7
7.) Observed Flows (No Meteorology)	411 *	69.4	±	34.2	78.1	±	35.8	86.8
[x] Steady Flows								
*Average of Variable Observed Flows								

DISCUSSION

Scaling Analysis

Dominant coastal circulation forcing mechanisms in the study area are determined here by considering the relative contributions of local, advective and Coriolis accelerations, bottom friction, and the baroclinic and barotropic pressure gradients. This is done by first applying a scaling analysis to the x- and y-momentum equations, and then through a relative order of magnitude analysis.

In a right-handed coordinate system, where x is aligned with the streamwise direction and is positive seaward, the tidally averaged momentum equations may be scaled to determine the dominant dynamics, as in Webb et al. (2007). Scaling and analyzing the contributions of the various terms' magnitudes (e.g. advective acceleration, Coriolis acceleration, local acceleration, and bottom friction) offers a quantitative comparison of their relative importance within the system. The equations used in the scaling analysis are given by Eqs. (16) and (17).

$$\left\langle u\frac{\partial u}{\partial x}\right\rangle + \left\langle v\frac{\partial u}{\partial y}\right\rangle + \left\langle w\frac{\partial u}{\partial z}\right\rangle - \langle fu\rangle = -\left\langle\frac{1}{p_o}\frac{\partial p}{\partial x}\right\rangle + \left\langle\frac{\partial}{\partial z}\left(A_v\frac{\partial u}{\partial z}\right)\right\rangle \tag{16}$$

$$\left\langle u\frac{\partial v}{\partial x}\right\rangle + \left\langle v\frac{\partial v}{\partial y}\right\rangle + \left\langle w\frac{\partial v}{\partial z}\right\rangle + \langle fv\rangle = -\left\langle\frac{1}{p_o}\frac{\partial p}{\partial y}\right\rangle + \left\langle\frac{\partial}{\partial z}\left(A_v\frac{\partial v}{\partial z}\right)\right\rangle \tag{17}$$

where f is the Coriolis parameter, p is pressure, A_v is vertical eddy viscosity, and $\langle\ \rangle$ is a time-averaging operator. Representative subtidal velocity (U,V), length (L_x,L_y), and depth (H) scales for the system are U~0.1 m s^{-1}, V~0.01 m s^{-1}, L_x~49000 m, L_y~26000 m, and H~ 3 m. It should be noted that L_x and L_y terms are averages across the entire study area.

This study utilizes ADCIRC's 2D depth integrated barotropic mode (i.e. all density gradients are assumed to be zero). Many estuaries along the northern Gulf of Mexico (including Mobile Bay) share several common attributes, including: shallow and wide basins, deep and narrow ship channels, diurnal tides with a micro-tidal exchange, and water exchange with the Gulf of Mexico via relatively narrow passes (Schroeder and Wiseman 1999). For such estuaries where stratification is common, this assumption may be problematic since density driven flows are neglected. The scaling analysis, presented in Table 5, demonstrates that the relative influence of the barotropic pressure gradient term is of the same order of magnitude as the baroclinic pressure gradient; however, the barotropic pressure gradient is approximately 3.5 times less than the baroclinic pressure gradient term. Local and advective terms are approximately 1 and 2 orders of magnitude less than both the friction and the Coriolis terms, respectively. It should be

noted that subtidal velocity measurements were obtained from Mobile
Container Terminal ADCP data; density information were obtained from
Meaher Park and Dauphin Island gauges (MBNEP/DISL); and water level
slope data were obtained from tide gauges at Mobile State Docks and
Dauphin Island. The measured values used in this scaling analysis
correspond to the period of the 30-day model validation for consistency. It is
acknowledged that the values presented in this scaling analysis do not sum to
zero, however, these values are presented here as an order of magnitude
analysis only.

Table 5: Scaling analysis of Eqs. (16). The canonical form of the drag coefficient is adopted, where C_d=0.0025. The local value of f is taken as f=7×10^{-5} s^{-1}. The representative density gradient is $\partial\rho/\partial x$=2 x 10^{-4} kg/m^3/m, and the reference density is ρ_o=1011.75 kg/m^3.

Term	Scaled Term	Value	Units
Local Acceleration	UU/L_x	2.04E-07	m/s/s
Advective Acceleration	VU/L_y	3.85E-08	m/s/s
Coriolis	fV	1.00E-06	m/s/s
Friction	$C_d U^2/H$	8.33E-06	m/s/s
Baroclinic PG	$1/\rho_o*\partial\rho/\partial x*gH$	6.98E-06	m/s/s
Barotropic PG	$g*\partial\eta/\partial x$	2.00E-06	m/s/s

A previous study has described estuary-Gulf exchange in Mobile Bay with
the use of a 3D baroclinic hydrodynamic model (Kim and Park 2012);
however, these studies have primarily focused on quantifying tidal exchanges

at Main Pass and Pass aux Herons with respect to water column stratification, freshwater input, and winds, and not the extensive responses of residence, exposure, and flushing times in Mobile Bay. While using a 3D baroclinic model will give more precise model estimations, the scope of this study is to determine the spatial and temporal responses of residence, exposure, and flushing times to riverine and meteorological forcing, and circulation at depth was not considered. Inclusion of baroclinic forcing would enhance circulation and therefore likely lower model predicted timescales; however, the use of a 3D model might increase predicted timescales by simulating stratification of the water column and vertical mixing during destratification events. Circulation at depth may be significant for Test Cases 2, 3, and 5 where stratification would likely occur due to relatively low discharge rates (Ryan et al. 1997; Park et al. 2007). However, this significance is likely only over a period of days and not over the timescales relative to this study (i.e. weeks or months). Furthermore, since the nature of this study is innovative and the results will help pioneer future studies, use of the 2D depth integrated barotropic model is an adequate approximation for now.

Bay Flushing: Riverine Dominated vs Tidally-Enhanced

Particle concentration (%) responses to the magnitude of steady, riverine discharge are analyzed to determine approximately when characterization of

bay flushing transforms from a tidally-enhanced to a riverine dominated system (Figure 26). Fluctuations in particle concentration are examined and a relationship to the magnitude of riverine discharge is inspected. This process is repeated with observed discharge data for Test Cases 6 and 7 to determine how the inclusion of meteorological forcing affects particle concentration curves and if steady, riverine test cases provide results which are comparable to observed variable discharge rates (Figure 27). Flushing times in Mobile Bay for each test case were previously summarized in Table 4.

Particle concentration (%) is calculated by dividing the instantaneous number of particles within the LPTM study area by the total number of initialized particles and is plotted against particle tracking time (days) for each steady flow test case (Figure 26). The frequency of model output is every three hours (eight times per day). All simulations had a minimum duration of 120 days with a 15 day ramp time. Where necessary, simulation durations were extended beyond 120 days to reveal the flushing time (i.e. particle concentration equal to or less than 36.79%) for each simulation. Percent and number of particles trapped at the end of each simulation are found in Table 6. More than 90% of the initialized 33,372 particles left the study area during each simulation, with the only exception being the minimum steady flow condition, Test Case 3, where approximately 20.2% of initial particles were trapped at the end of the simulation.

Table 6: Summarizes Mobile Bay, Alabama LPTM simulation results of percent (%) and number (#) of initial particles trapped during model simulations

Test Case	Discharge (m^3s^{-1})	% Paricles Trapped	# Particles Trapped
1.) Maximum	6747 [x]	2.8	932
2.) Mean	1715 [x]	5.8	1933
3.) Minimum	246 [x]	20.1	6717
4.) Wet Season	2637 [x]	5.3	1772
5.) Dry Season	802 [x]	7.1	2358
6.) Observed Flows (Full Meteorology)	637 *	2.6	532
7.) Observed Flows (No Meteorology)	411 *	6.9	2303
[x] Steady Flows			
*Average of Variable Observed Flows			

Observed concentration curves for Test Cases 1, 2, and 4 follow similar behavior, and each simulation achieves a flushing time concentration (i.e. particle concentration fell below 36.79% of initial concentration) in the first sixteen particle tracking days (Figure 26). The similar behavior observed for Test Cases 1, 2, and 4 suggest bay flushing can be characterized as riverine dominated for the respective flow conditions. Minor oscillations in particle concentration are observed in Test Cases 3 and 5 on a time scale of approximately one day. The increase in observed particle concentration can be attributed to the re-addition of particles that may have left the system during a previous ebb tide, but return during a flood tide (i.e. bay flushing characterized as tidally-enhanced). These oscillations become less obvious for Test Cases 1, 2, and 4 as the steady, riverine discharge is increased (Figure

65

26), suggesting that for Test Cases 3 and 5 bay flushing can be characterized as tidally-enhanced. However, the slope of the particle concentration curve for Test Case 5 follows a similar trend to Test Cases 1, 2, and 4; although, oscillations in particle concentration are still observed (Figure 26). It appears Test Case 5 constitutes a combination of a tidally enhanced and riverine dominated system with a low enough discharge to still feel the effects from tidal forcing. This is not so for Test Case 3, where oscillations are much more pronounced and the particle concentration curve does not behave similar to other test cases (Figure 26). Test Case 3 (i.e. 246 $m^3 s^{-1}$) decay of particle concentration is a function of tidal forcing with little influence from riverine discharge. Therefore, in terms of discharge, the bay changes from a tidally enhanced to a riverine dominated system approximately between the minimum discharge condition, Test Case 3 (i.e. 246 $m^3 s^{-1}$) and discharge rates near the dry season flow condition, Test Case 5 (i.e. 802 $m^3 s^{-1}$). Observed daily discharge for hindcast simulations, Test Cases 6 and 7, averaged 637 $m^3 s^{-1}$ and 411 $m^3 s^{-1}$. That suggests over the period of simulation the bay generally functions as a tidally enhanced system, except when exposed to discharge rates greater than Test Case 5 (i.e. 802 $m^3 s^{-1}$) for some extended duration. It should be noted in order to reach a flush time concentration, Test Case 3 was extended from 120 days to 180 days (Figure 26).
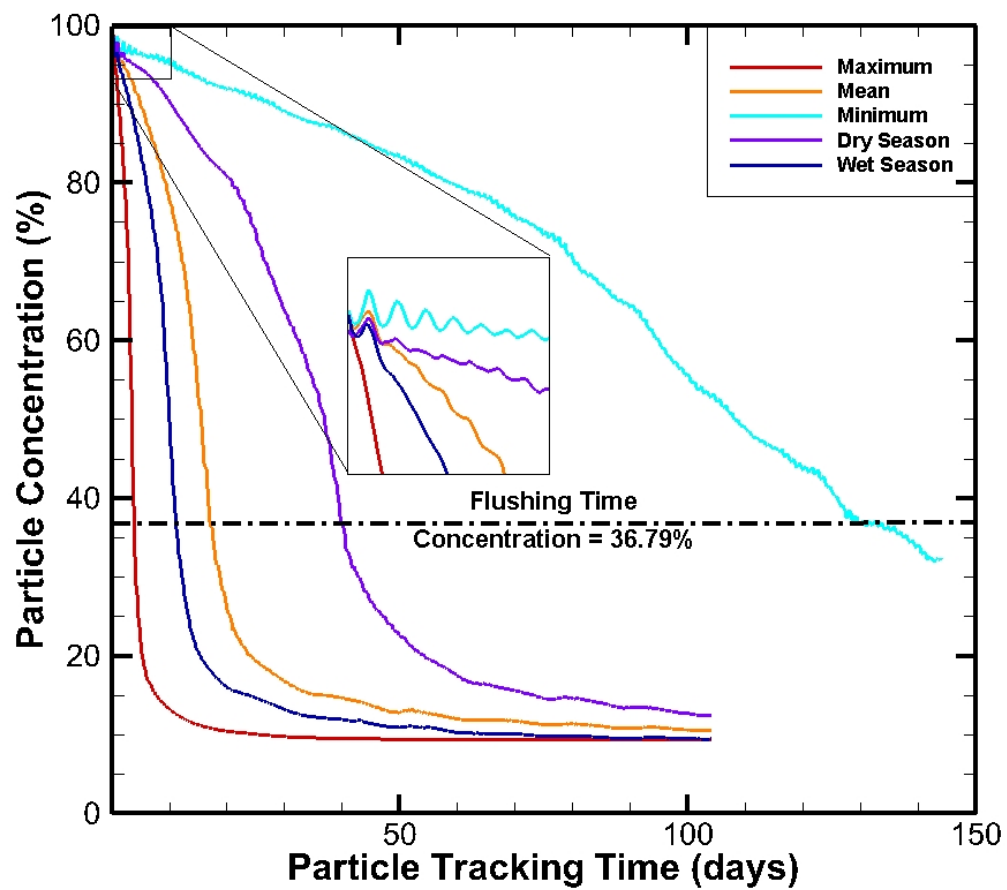
Figure 26: Particle concentration (%) plotted as a function of LPTM particle tracking time (days).

Observed discharge ($m^3 s^{-1}$) and particle concentration (%) are plotted against particle tracking time (days) for Test Cases 6 and 7 (Figure 27). In general, particle concentration decreases over time; however increases in concentration are observed for Test Case 6, where meteorology is included. These increases in concentration appear during periods of relatively low discharge (i.e. discharge magnitudes less than mean steady, riverine discharge, 1715 $m^3 s^{-1}$), so it is possible they are similar to the observed oscillations for Test Cases 3 and 5 and can be attributed to flood and ebb tide particle propagation. However, since Test Case 6 includes meteorological forcing they could also be associated to periods of southerly winds (i.e. those originated from south of the study area) that potentially propagate removed particles back into the system. Such wind forcing is typical for the period simulated as previously mentioned.

Particle concentrations respond more significantly to increases in discharge when meteorological forcing is not included in simulation, as seen at approximately particle tracking day 100 (Figure 27). Particle concentration abruptly decreases for both Test Cases 6 and 7 as the discharge rate begins to rise towards a peak rate of approximately 3500 $m^3 s^{-1}$; however, a steeper decrease in concentration for Test Case 7 is observed. The variation in concentration profiles between the two cases shows the significance of meteorological forcing with relation to circulation in Mobile Bay. Steep decreases in concentration are observed between approximately particle

68

tracking days 50 – 80 during Test Case 6 (Figure 27), which are not observed for Test Case 7. It should be noted that particle tracking days 50 – 80 approximately correspond to August 2011 – September 2011. During this time Tropical Storm Lee, with estimated peak wind speeds of approximately 50 knots, made landfall on September 4, 2011 in Louisiana before moving north-northeast towards Alabama and Mobile Bay (Brown 2011). Since riverine forcing magnitudes are identical for Test Cases 6 and 7, this discrepancy can be qualified to the inclusion of meteorological forcing for Test Case 6, and the steep decay in particle concentration for Test Case 6 is a direct result of strong wind fields observed during Tropical Storm Lee. Rainfall amounts associated with Tropical Storm Lee and its remnants also totaled as much as 32 cm in Mobile, Alabama from September 2, 2011 – September 10, 2011 (Brown 2011). Large amounts of rainfall continue throughout the watershed for several days as the storm continues to track north-northeast, and high discharge rates are observed as a result of this rainfall near particle tracking day 100 (Figure 27). It is interesting to note that the response of percent concentration to changes in riverine discharge for Test Case 7 (Figure 27), appears to lag similar in magnitude to a lag relationship for water to reach the bay from river gauging stations established by Schroder and Lysinger (1979) (e.g. 5 – 9 days).

When riverine discharge is the primary forcing mechanism, particle concentration profiles demonstrate Mobile Bay's transformation from a

tidally-enhanced to a riverine dominated system at discharge rates of approximately 802 $m^3 s^{-1}$ (Figure 26 and Figure 27). Equally near steady decreases in particle concentration are observed for Test Cases 1, 2, and 4 (Figure 26), where steady, riverine discharge rates are all over 802 $m^3 s^{-1}$. Similar behavior is observed during Test Case 7 when riverine discharge rates remain greater than 802 $m^3 s^{-1}$ over a period of multiple days (Figure 27). This behavior agrees with observations from steady, riverine discharge test cases, where Mobile Bay is demonstrated to transition from a tidally-enhanced to a riverine dominated system at discharge rates near the dry season flow condition (i.e. 802 $m^3 s^{-1}$).
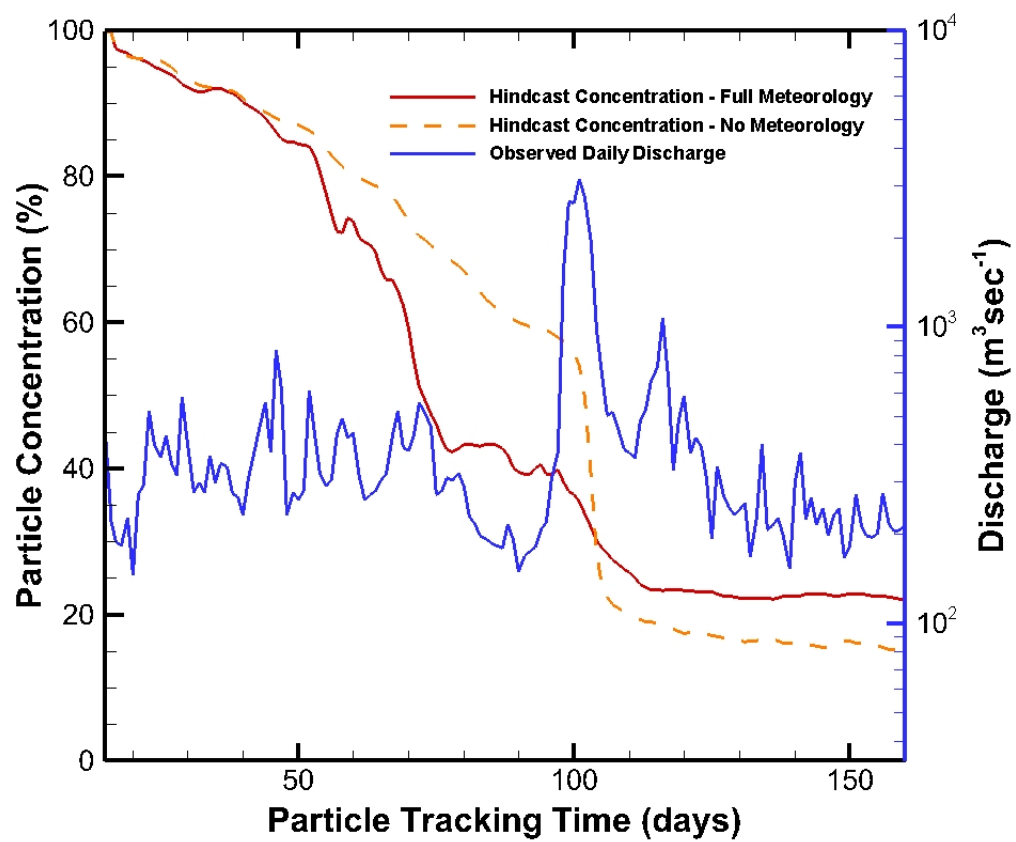
Figure 27: Particle concentration (%) plotted as a function of LPTM particle tracking time (days) for hindcast simulations.

Fourier analysis is used to identify periodic structures based on the time-series of particle concentration data from each steady, riverine discharge test case (Figure 28 (a)-(f)). Distinct tidal frequencies are observed on orders of once and twice per day, representing the principle tidal constituents (e.g. M_2, S_2, N_2, T_2, L_2, K_1, O_1, P_1, and Q_1). Tidal influences are generally observed for each test case at a frequency of once per day; however, Test Case 1 (Maximum) is an exception, where little to no increase in frequency magnitude is observed at any discrete frequency. Tidal influences at a frequency of once per day become less significant when steady, riverine discharge is greater than 1715 m^3 s^{-1} (Figure 28 (a)-(f)). This behavior generally agrees with observations from particle concentration profiles, where analysis reveals a distinction between a tidally-enhanced and riverine-dominated system in Mobile Bay at approximate discharge rates representative of the dry season flow condition (802 m^3 s^{-1}) (Figure 26). Furthermore, observations of particle concentration curves from hindcast simulation Test Cases 6 and 7 also agree with this behavior, where similar rates of particle concentration decrease to those observed for steady, riverine discharge test cases are observed when discharge rates remains greater than 802 m^3 s^{-1} on a time scale of multiple days. It should be noted that influences at a frequency of twice per day are only noticeably observed for Test Cases 2 and 5 (Figure 28), where steady, riverine discharges were 1715 and 2637 m^3 s^{-1}, respectively.
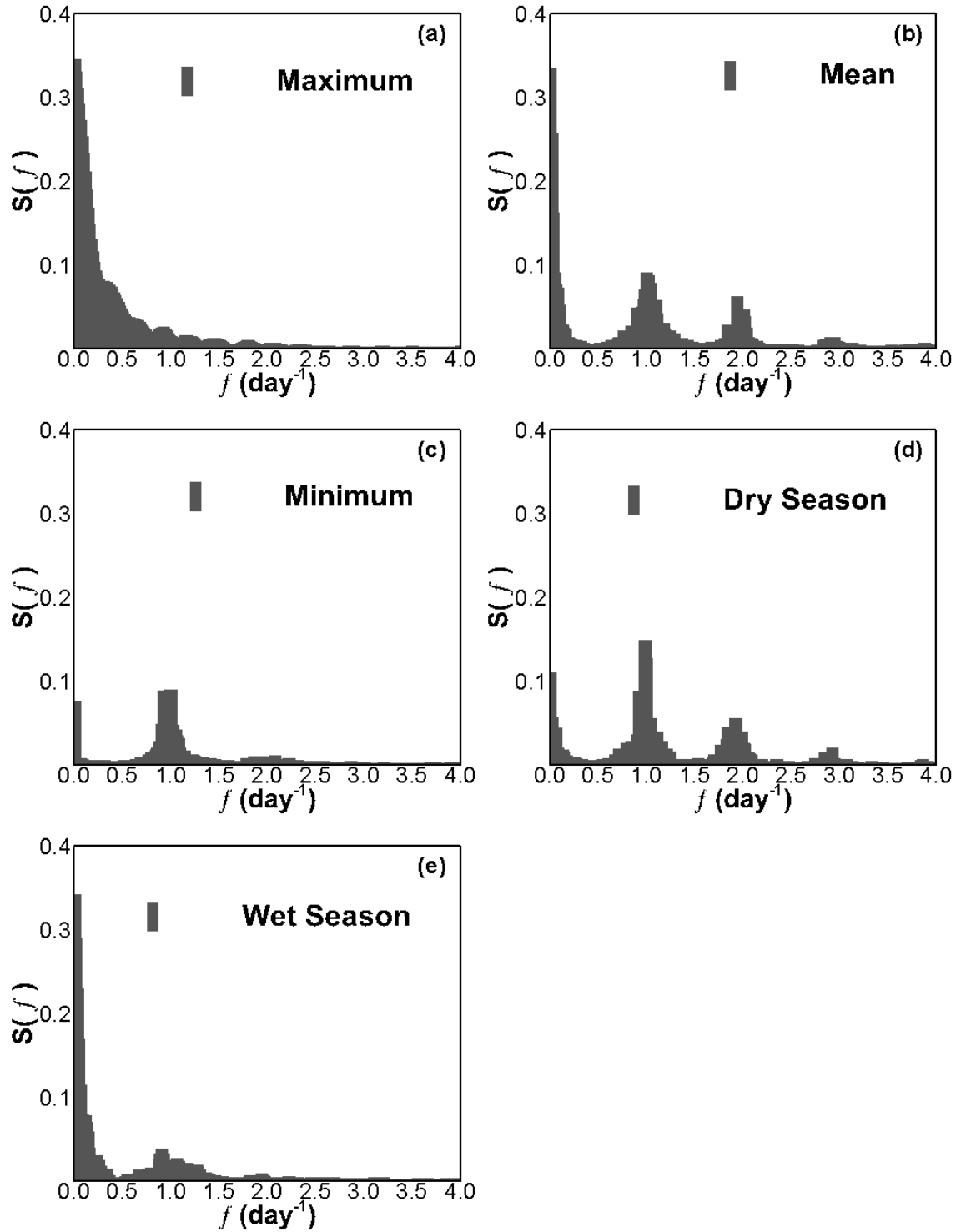
Figure 28: Frequency spectra comparison from a Fourier transform analysis of time-series concentration data for maximum (a), mean (b), minimum (c), dry season (d), and wet season (e) flow conditions.

A multiple regression ANOVA test is used to determine the relationships between steady, riverine discharge rates and predicted values of exposure, flushing, and residence times. The strongest relationship is observed between discharge rates and predicted residence times (p=0.17) when compared to exposure and flushing time predictions at a 95% confidence interval (p=0.19 and p=0.24, respectively). It should be noted that the sample size of flow conditions tested is relatively small (N=5). Correlation analysis of meteorological parameters (i.e. wind speed, wind direction, and flow conditions) and Test Case 6 (including full meteorological forcing) particle concentration results shows that particle concentration responses are most associated with changes in wind speed magnitude. Further details on routine statistical analysis can be found in Appendix A.

Model Predicted Flushing Time vs. Freshwater Fraction Method

Flushing times are plotted as a function of riverine discharge (Figure 29). Data are fit by power law using a least square regression to show correlations, as in Huang and Spaulding (2002). A power fit equation and average observed flows are employed to compare steady, riverine discharge flushing time estimates and those predicted by the model using variable observed flows. Model predicted flushing times are further compared to flush time calculations using the freshwater fraction method (Dyer 1973).

Model estimates of flushing times showed an inverse relationship to the magnitude of steady, riverine discharge. For example, as steady flow conditions increases from minimum to maximum flow conditions (i.e. 246 m^3 s^{-1} to 6747 m^3 s^{-1}), the average flushing time decreases by 127.9 days (Table 4). Least square regression fitting by power law show good correlation, with R^2=0.999, between flushing time and discharge (Figure 29). Average observed flows from Test Cases 6 and 7 are 637 m^3 s^{-1} and 411 m^3 s^{-1}, respectively. Note that the average observed flows are different here because of the duration of the hindcast simulations for each test case. In many ways, this is an inaccurate comparison; however, the values are compared to, not included in, the regression analysis for comparison purposes only. When employing these averaged observed flows for Test Cases 6 and 7, the power fit equation yields flushing times of approximately 51 and 81 days, respectively. The model predicted flushing times for Test Cases 6 and 7 are 82.8 and 86.7 days. The power fit equation predicts a flushing time for Test Case 7 that is reasonably close to model results, but underestimates the flushing time for Test Case 6 where meteorological forcing is included.

The power law formula underestimates the simulated flushing time by approximately 62%. In the case of the hindcast without meteorological forcing, the power law formula underestimates the simulated flushing time by only about 7%. It is therefore evident, that prediction of the flushing time is far more sensitive to the local winds than it is the variable, daily riverine

discharge. These results suggest that the local meteorological forcing may account for as much as 55% (62% - 7%) of the variability of flushing times from those predicted by the regression equation based on steady discharge. The freshwater fraction method (Dyer 1973) generally underestimates flushing times in Mobile Bay, Alabama (Table 7). In all cases, the freshwater fraction method estimates flushing times that are almost one-half the model predicted flushing times. The flushing time is also calculated without the inclusion of the Frac$_{FW}$ term in Equation 10 for further analysis, so that flushing time is simply defined as the estuarine volume divided by the freshwater inflow for each case. Flushing time estimates are remarkably close to model predictions but generally overestimate flushing times when employing this method (Table 7). It should be noted that the freshwater fraction method results are dependent upon assumed values for average estuarine and ocean salinity, and modifying these assumptions would alter these estimates. Average assumed salinities in Mobile Bay for this study are consistent with Pennock et al. (1994).

The freshwater fraction method has been used to describe mean estuarine flushing capacities (Huang and Spaulding 2002; Huang 2007; Sheldon and Alber 2002; Shedon and Alber 2006; Regnier and O'Kane 2004), and is considered to give reliable estimations of flushing times, although modest underestimates have been recognized (Sheldon and Alber 2006). However, in

many cases, such as when flushing time is used to evaluate the potential flushing of pollutants, a more conservative estimate would be preferred (Sanford et al. 1992). For this reason, discrepancies in flushing time estimations between the model predictions and the freshwater fraction method should be further investigated to ensure appropriate estimates are used in management practices.

Previous studies on physical mass transport of water in Mobile Bay (Austin 1954; Wiseman et al. 1988) have estimated the flushing time at 50 days and 20 days, respectively. It should be noted that Wiseman et al. (1988) came to that estimate by assuming a mean velocity through the upper layers of Main Pass, and Austin (1954) by using a modified tidal prism technique. The Austin (1954) estimated timescale is based on a six day long survey of Mobile Bay conducted in October, 1952, and only consider a freshwater discharge of approximately 382 $m^3 s^{-1}$. The model predicted flushing time for this flow condition using the power law formula developed from steady riverine test case results is approximately 82 days, and therefore, the Austin (1954) flushing time estimate of 50 days is an underestimate of approximately 60% of the model predicted flushing time. The freshwater discharge considered by Wiseman et al. (1988) is unknown; however, Wiseman et al. (1988)'s estimate of 20 days generally agrees with results from Test Case 2 (i.e. mean flow conditions), where the flushing time was

predicted to be 17.2 days. It should be noted that the definition of flushing time used by Wiseman et al. (1988) and Austin (1954) is unknown.
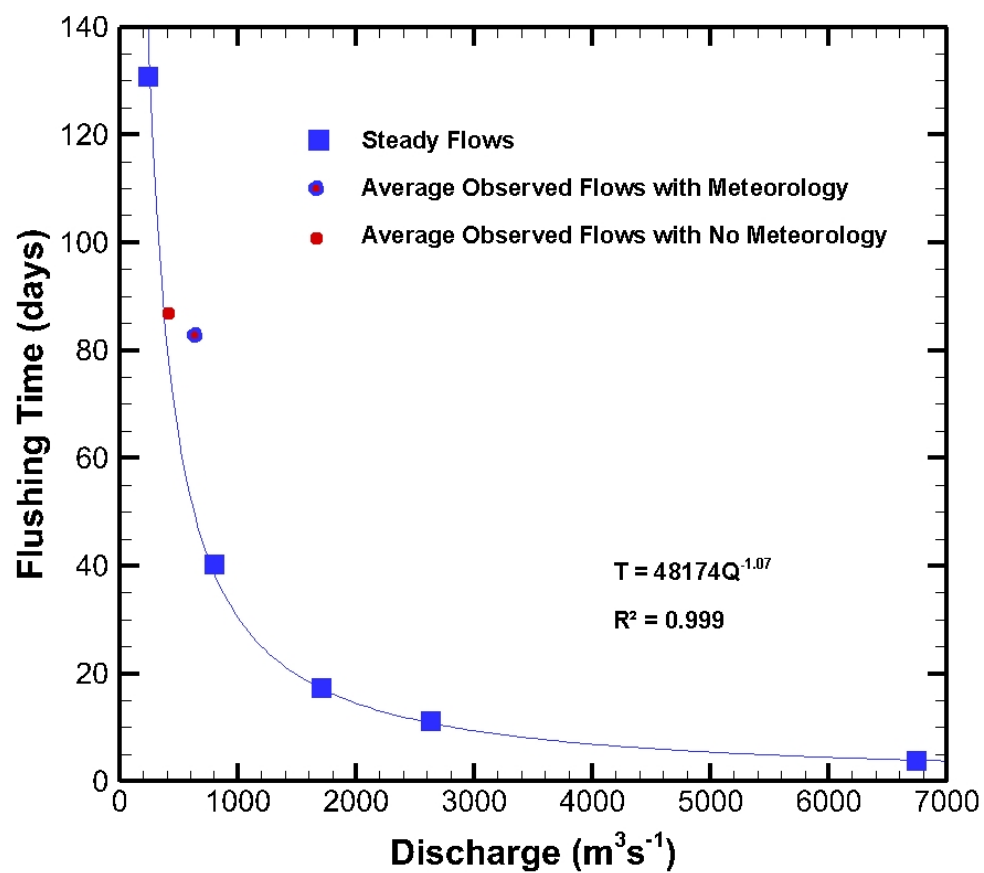
Figure 29: Model predicted flushing times in Mobile Bay, Alabama. A least-square regression line is fit by power law.

Table 7: Comparison of model predicted and freshwater fraction method calculated flushing times in Mobile Bay, Alabama.

Test Case	Discharge (m^3s^{-1})	Model Predicted Flushing Time (days)	Freshwater Fraction Method with $Frac_{FW}$ (days)	Freshwater Fraction Method without $Frac_{FW}$ (days)
1.) Maximum	6747 [x]	3.8	2.4	5.5
2.) Mean	1715 [x]	17.2	9.4	21.6
3.) Minimum	246 [x]	130.7	65.2	150.6
4.) Wet Season	2637 [x]	11.2	6.1	14.0
5.) Dry Season	802 [x]	40.2	20.0	46.2
6.) Observed Flows (Full Meteorology)	637 *	82.7	25.2	58.1
7.) Observed Flows (No Meteorology)	411 *	86.8	39.0	90.1
[x] Steady Flows				
*Average of Variable Observed Flows				

Spatially Averaged Exposure and Residence Timescales

Spatially averaged exposure and residence timescales are plotted as a function of steady, riverine discharge (Figure 30 and Figure 31, respectively). Data are fit by power law using a least square regression to show correlations. A power fit equation and average observed flows are employed to compare steady, riverine discharge estimates of exposure and residence times and those predicted by the model for variable observed flows.

In general, spatially averaged exposure and residence times showed an inverse relationship to the magnitude of steady, riverine discharge. For example, as steady flow conditions increases from 1715 $m^3\,s^{-1}$ to 6747 $m^3\,s^{-1}$,

the average residence time decreases by 11.5 days (Table 4). Least square

regression fitting by power law show good correlation, with $R^2 = 0.998$,

between residence time and discharge (Figure 31). Exposure time and

discharge also show good correlation, with $R^2 = 0.998$ (Figure 30). Average

observed flows from Test Cases 6 and 7 are 637 $m^3 s^{-1}$ and 411 $m^3 s^{-1}$,

respectively. When employing these averaged observed flows for Test Cases 6

and 7, the power fit equation yields residence times of approximately 41.2

and 55.9 days, respectively. The model predicted residence times for Test

Cases 6 and 7 were 76.0 and 69.4 days, respectively. Likewise, when

employing these averaged observed flows for Test Cases 6 and 7, the power fit

equation yields exposure times of approximately 51.1 and 68.6 days,

respectively. The model predicted exposure times for Test Cases 6 and 7 were

83.4 and 78.1 days, respectively. Regression is based on the steady, riverine

discharge results, and Test Cases 6 and 7 are shown here for comparison

purposes only. It should be noted that wide ranging spatial variability in

timescales was observed for each test case, and estimating a singular value to

represent these timescales across the entire study area can be misleading, as

discrete areas of the bay behave differently.

Estimates of residence time in Mobile Bay to be used for comparative

analysis is lacking in the published literature. Pennock et al. (1994) gives an

estimate of the average freshwater residence time in Mobile Bay equal to 17

days for an average discharge of 2245 $m^3 s^{-1}$ (Anon 1989). This value

generally agrees with the model predicted spatially averaged residence time for Test Case 2 (i.e. 1715 m^3 s^{-1}) of 17.1 days; however, the Anon (1989) estimate of freshwater residence time is an overestimate compared to the model predicted spatially averaged residence time employing the power fit equation for a discharge of 2245 m^3 s^{-1}. It should be noted that the definition of freshwater residence time and the method used to determine the freshwater residence time by Anon (1989) is uncertain.
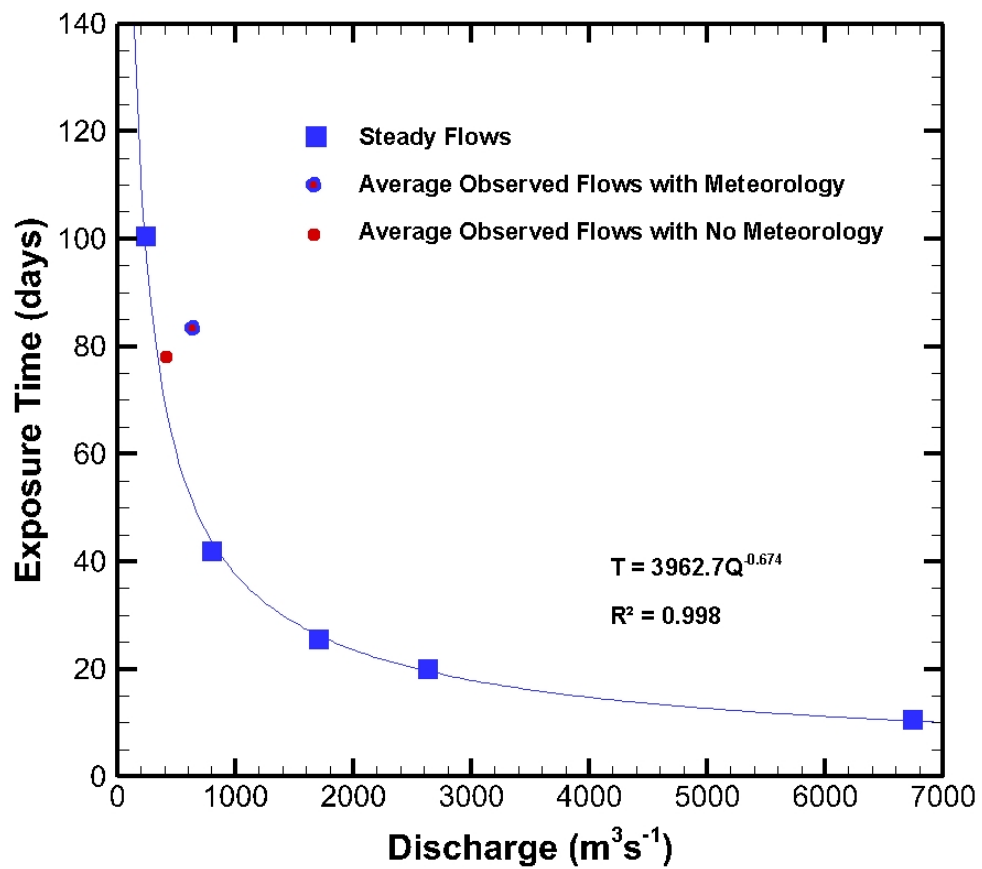
Figure 30: Model predicted exposure times plotted versus discharge. A regression line was fit by the power law.
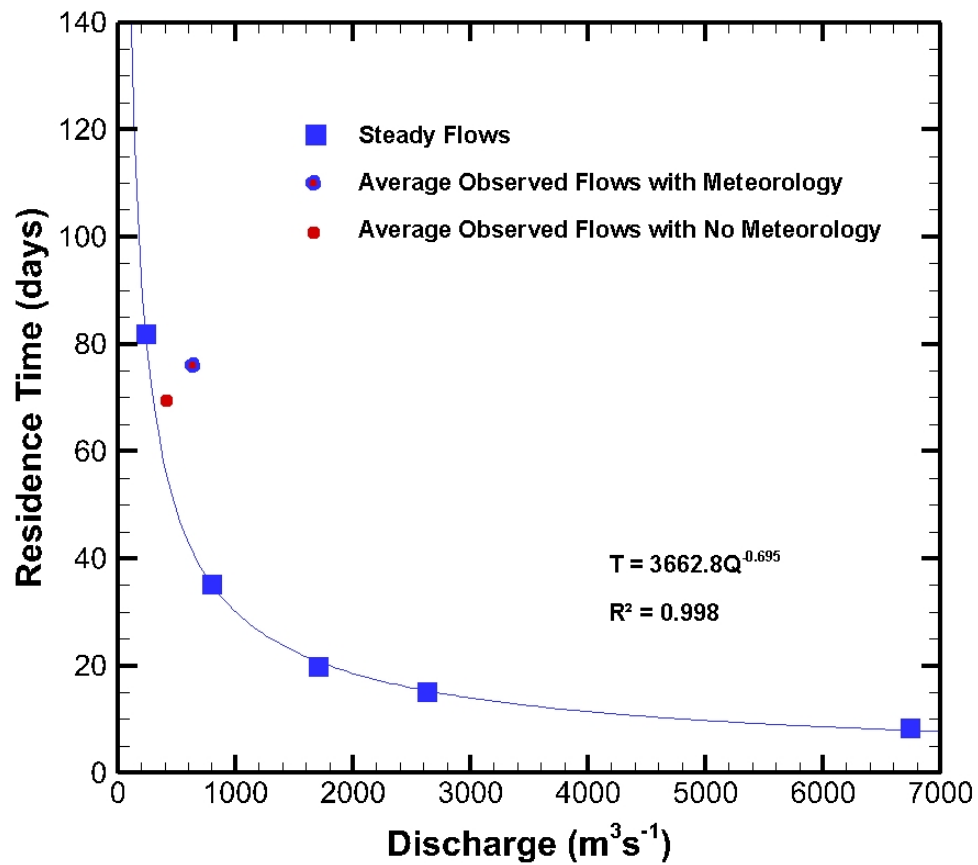
Figure 31: Model predicted residence times plotted versus discharge. A regression line was fit by the power law.

Synoptic Map of Spatial Variability in Timescales

A synoptic map is generated from synthesizing spatial variability of exposure and residence time for all seven test cases (Figure 32). Spatial variability maps for each test case are examined by contouring results at various intervals. Mobile Bay is divided into five zones based on the ability to flush water from the system (i.e. excellent flushing is synonymous with the shortest residence and exposure times) (Figure 32). Results show the exposure, flushing, and residence timescales are responsive to the magnitude of riverine discharge.

Consistent with northern hemisphere conditions, river waters favor the western shore as they move to the south while Gulf of Mexico waters favor the eastern shore as they move to the north (Schroeder 1978). This behavior is reflective in the synoptic map where better flushing is observed along the western shore than the eastern shore (Figure 32). Areas of exception are observed in the northwest section of the bay and in the Mobile-Tensaw delta, where long timescales and poor flushing are observed for all seven test cases.

Shorter timescales are observed near the GIWW for all test cases. It should be noted that shorter timescales observed near the GIWW for Test Case 6 (including meteorological forcing) are not as distinct as for other test cases, and meteorology has an effect on timescales, as observed when comparing Figure 24 and Figure 25. Relatively long timescales are observed along the mid-section of Bon Secour Bay for each test case; however, this

observation is less obvious with the inclusion of meteorological forcing. The behavior of particles initialized in Bon Secour Bay behave nearer to homogeneous conditions for Test Case 6, and no clear division of timescale magnitude can be made throughout Bon Secour Bay as in other test cases. Wind forcing tends to overwhelm tidal forcing in this region of the bay. The effects of river forcing are most notable to the west of the ship channel, as demonstrated by the almost static nature of contour intervals along the eastern shore and within Bon Secour Bay. Nevertheless, relatively long timescales are observed throughout Bon Secour Bay for all test cases, and this area is assumed to exhibit areas of relatively poor flushing.

Dauphin Island affects flushing by separating inward and outward flow from the estuary at Main Pass and Pass aux Herons. The effects are observed by the "dip" in flushing capacity for Zone 1 near the southwest (lower-left) section of the bay (Figure 32). In general, better flushing is observed near Main Pass than Pass aux Herons. This behavior is predictable since Main Pass accounts for most of Mobile Bay's estuary-gulf exchange (Schroeder 1978; Dinnel et al. 1990; Kim and Park 2012).
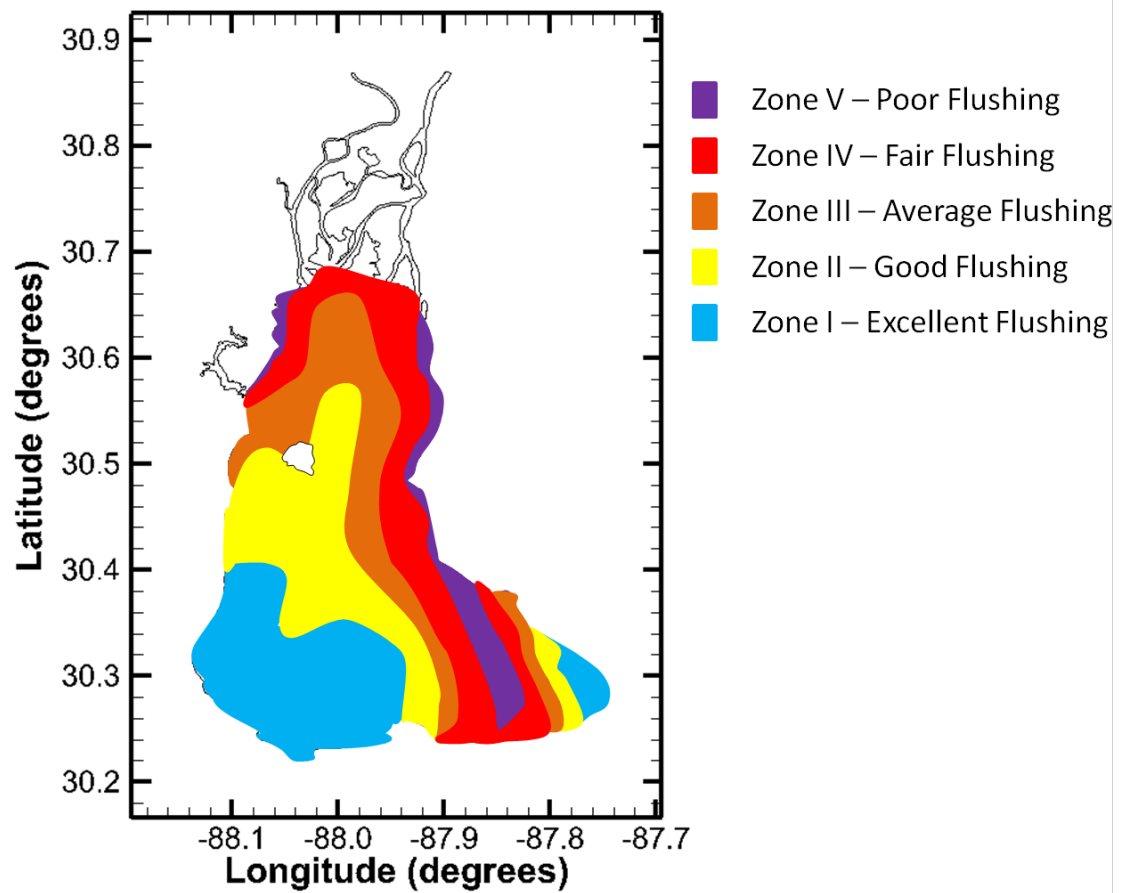
Figure 32: Synoptic map of zones representing the Bay's flushing capacity generated using LPTM output of timescale spatial variability.

CONCLUSIONS

This study provides an innovative study of hydrodynamic timescale
response to riverine discharge in Mobile Bay, Alabama. These timescales can
be used to demonstrate the rate of removal for pollutants, contamination and
nutrient levels, distributions of organisms, and the spatio-temporal
variations of each of these in bays and estuaries. Previous studies into the
behavior of these timescales in Mobile Bay are limited, and this study's
application of a sophisticated hydrodynamic model, ADCIRC, to quantify
these descriptive variables is unique.

The response of hydrodynamic timescales to riverine discharge in Mobile
Bay, Alabama is found to vary spatially with respect to initial position in the
estuary. This study's results meet the primary objective, to estimate the
residence, exposure, and flushing times for Mobile Bay, Alabama using
two-dimensional hydrodynamic advanced circulation model output. The
following list is a summary of pertinent results from this study of Mobile Bay,
Alabama.

- Timescales vary spatially throughout the entire study area of
  Mobile Bay, and therefore, it is difficult to associate one value with

timescales for the entire Bay. Timescales range from 1 to more than 200 days in Mobile Bay with standard deviations of 20 to 40 days.

- Mobile Bay likely is generally characterized as a riverine-dominated system at freshwater discharge rates greater than approximately 802 $m^3\,s^{-1}$.

- Meteorology is important to transport processes, and the subsequent hydrodynamic timescales, due to the shallow nature of the Bay.

- Areas of poor flushing include: Bon Secour Bay, the eastern shoreline of Mobile Bay, and the Mobile-Tensaw Delta.

Model predicted flushing times for Mobile Bay ranged from approximately 4 to 130 days under steady, riverine maximum and minimum flow conditions (i.e. 6747 and 246 $m^3\,s^{-1}$, respectively). Comparative analysis of flushing time calculations using the freshwater fraction method (Dyer 1973) yield relatively similar estimates to model predicted flushing times when not employing the $Frac_{FW}$ term in Equation 10, and therefore, the flushing time is simply defined as the estuary volume divided by freshwater inflow. Again it should be noted that wide ranging spatial variability in timescales was observed for each test case, and estimating a singular value to represent these timescales across the entire study area can be misleading. It is therefore difficult to

consider one timescale value to represent the entire bay, and estimates based on the methods such as the freshwater fraction method can be ambiguous.

Coastal bays and estuaries are complex systems where bathymetry, fresh riverine discharge, tides, and winds can greatly influence estuarine dynamics. An estuary can operate primarily as a function of any one or multiples of these parameters depending on their relative magnitudes. In general, Mobile Bay functions as a tidally-enhanced system when riverine discharge rates are near or below approximate flow conditions representative of Test Case 2 (i.e. 802 m^3 s^{-1}) and meteorological forcing is not considered. When discharge rates from the Alabama and Tombigbee rivers are greater than 802 m^3 s^{-1} tidal influences weaken and the bay primarily functions as a riverine dominated system.

Hindcast simulations of observed discharge rates and tides demonstrate the important role meteorology has on the circulation of the shallow waters in Mobile Bay. Sustained south winds can propagate removed particles back into the bay, and sustained north winds can successfully drive surface currents southward removing particles from the estuary. Statistical analysis shows that changes in particle concentration within the study area are most correlated to changes in wind speed compared to changes in parameters such as freshwater discharge and changes in wind direction. However, since only one test case included meteorological forcing, this relationship should be subjected to a more thorough analysis.

In general, average to excellent flushing is observed throughout much of Mobile Bay. Areas of relatively poor flushing include the mid-section of Bon Secour Bay, along the eastern shoreline of Mobile Bay, and in the Mobile-Tensaw Delta. Poor flushing observed in the eastern portions of the Bay is likely attributed to the influence of gravitational circulation in the horizontal plane (i.e. the influence of Coriolis), and perhaps the interaction between tides, river input, and the shallow nature of the north part of the Bay. Poor flushing and long timescales in the Mobile-Tensaw Delta may be partially attributed to the Highway 90 Causeway across the southern terminus of the Delta, but further investigation is required.

Previous studies regarding the extensive circulation of Mobile Bay are lacking, and to the author's knowledge only three published estimates related to hydrodynamic timescales in Mobile Bay exist. Even though comparative results are limited, the published timescales compared to this study's results generally underestimate timescales in Mobile Bay. However, it should be noted that, in some cases, detailed methodology and computational values for these studies is uncertain. The range of model predicted timescale estimates presented within are more accurate characterizations of extensive estuary dynamics in Mobile Bay than previous study estimates due to the high degree of resolution and advanced nature of technology utilized in computation.

RECOMMENDATIONS

While the research presented is adequate to describe the extensive behavior of hydrodynamic timescales in Mobile Bay, further research should consider the effects of meteorological forcing during simulations. Study results show this inclusion to be important in the behavior of hydrodynamic timescales, particularly in shallow areas. Regions of poor flushing should be investigated as their influence on water quality could be significant. Future studies should also attempt to further describe the correlation of hydrodynamic timescales and particular forcing parameters to more accurately establish predictive relationships. Further consideration should be given to the comparative analysis of model predicted flushing times and estimates using the freshwater fraction method, specifically the discrepancy among results. Finally, an appropriate suite of model simulations should consider the effects of stratification and gravitational circulation on hydrodynamic timescales, particularly for low discharge magnitudes and weak meteorological forcing, through application of a comprehensive 3D baroclinic model.

REFERENCES

REFERENCES

Aikman, F., and Lanerolle, L.W.J. (2005). "Report on the NOS Workshop on Residence/Flushing Times in Bays and Estuaries." NOAA Technical Report NOS CS 20, NOAA, Silver Spring, Maryland.

Anonymous. (1989). "Strategic assessment of near coastal waters. Susceptibility and status of Gulf of Mexico estuaries to nutrient discharges." – Summary Rep. NOAA/EPA Team on Near Coastal Waters.

Austin, G.B. (1954). "On the circulation and tidal flushing of Mobile Bay, Alabama. Part 1." Texas A&M College Research Foundation Project 24, Technical Report 12, College Station, Texas.

Atkinson, A., Siegel, V., Pakhomov, EA., and Rothery, P. (2004). "Longterm decline in krill stock and increase in salps within the Southern Ocean." Nature 432, 100-103.

Blumberg, A.F., and Mellor, G.L. (1987). "A Description of a Three-Dimensional Coastal Ocean Circulation Model." Three Dimensional Coastal Ocean Models, American Geophysical Union, Washington, DC, 1-16.

Blumberg, A.F., Dunning, D.J., Li H., Heimbuch D., and Geyer, W.R. (2004). "Use of a particle-tracking model for Predicting Entrainment at Power Plants on the Hudson River." Estuaries, 27(3), 515-526.

Boyton, W.R., Garber, J.H., Summer, R., and Kemp, W.M. (1995). "Inputs, transformations, and transport of nitrogen and phosphorus in Chesapeake Bay and selected tributaries." Estuaries, 18, 285-314.

Brown, D.P. (2011). "Tropical Cyclone Report Tropical Storm Lee." Rep. No. AL132011, National Hurricane Center, Miami, Florida

Burwell, D., Vincent, M., Luther, M., and Galperin, M. (2000). "Modeling Residence Times: Eulerian vs. Lagrangian." Estuarine and Coastal Modeling, ASCE, Reston, Virginia. 995-1009.

Cameron, W.M., and Pritchard, D.W. (1963). "Estuaries." The Sea: Ideas and Observations on Progress in the Study of the Seas. Volume 2: The Composition of Sea-Water, Comparative and Descriptive Oceanography. New York, New York, 305-324.

Creel, L. (2003). "Ripple Effects: Population and Coastal Regions." Population Reference Bureau Measure Communication. Washington, DC.

Dietrich, J.C., Trahan, C.J., Howard, M.T., Fleming, J.G., Weaver, R.J., Tanaka, S., Yu, L., Luettich Jr. R.A., Dawson, C.N., Westerink, J.J., Wells, G., Lu, A., Vega, K., Kubach, A., Dresback, K.M., Kolar, R.L., Kaiser, C., and Twilley, R.R. (2012). "Surface trajectories of oil transport along the Northern Coastline of the Gulf of Mexico." Continental Shelf Research, 41, 17-47.

Dinnel, S.P., Schroeder, W.M., and Wiseman, W.J. (1990). "Estuarine-Shelf Exchange Using Landsat Images of Discharge Plumes." Journal of Coastal Research, Fort Lauderdale, Florida, 789-799.

Dyer, K.R. (1973). Estuaries: A Physical Introduction, 1st edition. John Wiley and Sons, London, England.

Dzwonkowski, B., Park, K., Ho, K.H., Graham, W., Hernandez, F., Powers, S. (2011). "Hydrographic variability on a coastal shelf directly influenced by estuarine outflow." Continental Shelf Research, 31, 939-950.

Guo, Q., and Lordi, G.P. (2000). "Method for quantifying freshwater input and flushing time in estuaries." Journal of Environmental Engineering, 126, 675-683.

Hagy, J.D., Sanford, L.P., and Boynton, W.R. (2000). "Estimation of net physical transport and hydraulic residence times for a coastal plain estuary using box models." Estuaries, 23(3), 328-340.

Huang, W., and Spaulding, M. (2002). "Modeling residence time response to freshwater input in Apalachicola Bay, Florida, USA." International Journal of Hydrological Processes, 16, 3051-3064.

Huang, W. (2007). "Hydrodynamic modeling of flushing time in a small estuary of North Bay, Florida, USA." Estuarine, Coastal, and Shelf Science, 74, 722-731.

Huh, O.K., Rouse, L.J., and Walker, N.D. (1984). "Cold-air outbreaks over the northwest Florida continental shelf: heat flux process and hydrographic changes." Journal of Geophysical Research, 89, 717-726.

Ketchum, B.H. (1951). "The exchanges of fresh and salt water in tidal estuaries." Journal of Marine Research, 10, 18-38.

Kim, C.-K., and Park, K. (2012). "A modeling study of water and salt exchange for a micro-tidal, stratified northern Gulf of Mexico estuary." Journal of Marine Systems, 96-97, 103-115.

Knoppers, B., Kjerfve, B., Carmouze, J.-P. (1991). "Trophic state and water turn-over time in six choked coastal lagoons in Brazil." Biogeochemistry, 14, 149-166.

Kolar, R.L., Gray, W.G., Westerink, J.J., and Luettich, R.A. (1994). "Aspects of Nonlinear Simulations Using shallow Water Models Based on the Wave Continuity Equation." Computers and Fluids, 23, 523-538.

Kuo, A.Y., and Neilson, B.J. (1988). "A modified tidal prism model for water quality in small coastal embayments." Water Science Technology, 20, 133-142.

Kuo, A.Y., Park, K., Kim, S.-C., and Lin, J. (2005). "A Tidal Prism Water Quality Model for Small Coastal Basins." Coastal Management, 33, 101-117.

Lauff, G. (1967). "Estuaries." American Association for the Advancement of Science, Pub. No. 83, Washington, D.C.

Lee, J.L., Webb, B.M., Dzwonkowski, B., Park, K., and Valle-Levinson, A. (2013). "Bathymetric influences on tidal currents at the entrance to a highly stratified, shallow estuary." Continental Shelf Research, 58, 1-11.

Luettich, R.A., Westerink, J.J., and Scheffner, N.W. (1992). "ADCIRC: An Advanced Three-Dimensional Circulation Model for Shelves, Coasts, and Estuaries." Theory and Methodology of ADCIRC-2DDI and ADCIRC-3DL, Report 1, Technical Report DRP-92-6, US Army Corps of Engineers, Washington, D.C.

Luketina, D. (1998). "Simple tidal prism models revisited." Estuarine Coastal and Shelf Science, 46, 77-84.

Meyers, S.D., and Luther, M.E. (2008). "A Numerical Simulation of Residual Circulation in Tampa Bay. Part 2: Lagrangian Residence Time." Estuaries and Coasts, 31, 815-827.

Miller, R.L., and McPherson, B.F. (1991). "Estimating estuarine flushing and residence times in Charlotte Harbor, Florida, via salt balance and a box model." Limnology and Oceanography, 36, 602-612.

National Research Council (2000). "Clean Coastal Waters: Understanding and Reducing the Effects of Nutrient Pollution." National Academy Press, Washington, D.C.

Park, K., Kim, C.-K., and Schroeder, W.W. (2007). "Temporal variability in summertime bottom hypoxia in shallow areas of Mobile Bay, Alabama." Estuaries Coasts, 30, 54-65.

Pennock, J.R., Sharp, J.H., and Schroeder, W.W. (1994). "What controls the expression of estuarine eutrophication? Case studies of nutrient enrichment in the Delaware Bay and Mobile Bay Estuaries, USA." Changes in fluxes in estuaries: implications from science to management, K.R. Dyer and R.J. Orth, eds., Denmark: Olsen & Olsen. 139-146.

Quinn, H., Tolson, J.P., Klien, C.J., Orlando, S.P., and Alexander, C. (1986). "Strategic Assessment of Near Coastal Waters, Susceptibility and Status of Gulf of Mexico Estuaries to Nutrient Discharges." Ocean Assessments Division, Office of Oceanography and Marine Assessments, National Ocean Service, NOAA, Rockville, MD.

Reed, M., Turner, C., and Odulo, A. (1994). "The role of wind and emulsification in modeling oil spill and surface drifter trajectories." Spill Science & Technology Bulletin, 1 (2), 143-157.

Regnier, P., and O'kane, J.P. (2004). "On the Mixing Process in Estuaries: The Fractional Freshwater Method Revisited." Estuaries, Vol. 27, No. 4, 571-582.

Ryan, H., Noble, M., Williams, E., Schroeder, W., Pennock, J., and Gelfenbaum, G. (1997). "Tidal current shear in a broad, shallow, river-dominated estuary." Continental Shelf Research, 17, 665-688.

Sanford, L.P., Boicourt, W.C., and Rives, S.R. (1992). "Model for estimating tidal flushing of small embayments." Journal of Waterway, Port, Coastal and Ocean Engineering, ASCE, 118, 635-654.

Schroeder, W.W. (1978). "Riverine influence on estuaries: a case study." Estuarine Interactions, M.S. Wiley, ed., Academic Press, New York, New York, 347-364.

Schroeder, W.W., and Lysinger, W.R. (1979). "Hydrography and circulation of Mobile Bay." Symposium on the Natural Resources of the Mobile Bay Estuary, H.A. Loyacano and J.P. Smith, eds., U.S. Army Corps of Engineers, Mobile District, Mobile, Alabama, 75-94.

Schroeder, W.W., and Wiseman, W.J. (1986). "Low-frequency shelf-estuarine exchange processes in Mobile Bay and other estuarine systems on the northern Gulf of Mexico." Estuarine Variability, D. Wolfe, ed., Academic Press, New York, New York, 355-367.

Schroeder, W.W., and Wiseman, W.J. (1999). "Geology and hydrodynamics of Gulf of Mexico estuaries." Biochemistry of Gulf of Mexico estuaries, T.S. Bianchi, J.R. Pennock, and R.R. Twilley, eds., John Wiley & Sons, New York, 3-28.

Sheldon, J.E., and Alber, M. (2002). "A comparison of residence time calculations using simple compartment models of the Altamaha River estuary, Georgia." Estuaries, 25, 1304-1317.

Sheldon, J.E., and Alber, M. (2006). "The Calculation of Estuarine Turnover Times Using Freshwater Fraction and Tidal Prism Models: A Critical Evaluation." Estuaries and Coasts, 29(1), 133-146.

Shen, J., and Haas, L. (2004). "Calculating age and residence time in the tidal York River using three-dimensional modal experiments." Estuarine, Coastal, and Shelf Science, 61, 449-461.

Signell, R.P., and Butman, B. (1992). "Modeling tidal exchange and dispersion in Boston Harbor." Journal of Geophysical Research, 97, 15591-15606.

Solis, R.S., and Powell, G.L. (1999). "Hydrography, mixing characteristics, and residence times of Gulf of Mexico estuaries." T.S. Bianchi, J.R. Pennock, and R.R. Twilley, eds., Biochemistry of Gulf of Mexico estuaries, John Wiley & Sons, New York, 29-61.

Swanson, J.C., and Mendelsohn, D. (1996). "BAYMAP, A simplified embayment flushing and transport model." M. Spaulding, and R. Cheng, eds., Proceedings of the Fourth International Conference on estuarine and Coastal Modeling, October 26-28, 1995, San Diego, CA.

Thomann, R., and Muller, J. (1987). Principles of Surface Water Quality Modeling and Control. Harper & Row, New York, 621.

Webb, B.M., King, J.N., Tutak, B., and Valle-Levinson, A. (2007). "Flow structure at a trifurcation near a North Florida inlet." Continental Shelf Research 27, 1528-1547.

Westerink, J.J., Bain, C.A., Luettich, Jr. R.A., and Scheffner, N.W. (1994). "ADCIRC: An Advanced Three-Dimensional Circulation Model for Shelves, Coasts, and Estuaries. User's Manual for ADCIRC-2DDI: Report 2." Technical Report DRP-92-6, US Army Corps of Engineers, Washington, D.C.

Wiseman, W.J., Schroeder, W.W., and Dinnel, S.P. (1988) "Shelf-Estuarine Exchanges between the Gulf of Mexico and Mobile Bay, Alabama." American Fisheries Society Symposium 3, 1-8.

Wolanski, E. (1994). "Physical oceanography process of the Great Barrier Reef." CRC Press, Boca Raton, Florida, 194.

Zimmerman, J.T.F. (1976). "Mixing and flushing of tidal embayments in the western Dutch Wadden Sea. Part I: Distribution of salinity and calculation of mixing time scales." Netherlands Journal of Sea Research, 10, 149-191.

APPENDICES

APPENDIX A: STATISTICAL ANALYSIS

Routine statistical analysis is performed to determine correlations between the daily averaged change in particle concentration for each test case and daily averages of parameters such as changes in riverine discharge magnitude, changes in wind speed, and changes in wind direction, as well as correlations between steady, riverine discharge magnitude and the model predicted timescales. The potential relationship between steady, riverine discharge magnitudes and model predicted timescales is further investigated by a multiple regression ANOVA test. Routine statistical analysis results are presented in the following section.

Table 8: Correlation coefficient analysis for change in flow magnitude (m^3 s^{-1}) and the changes in particle concentration (%) for Test Case 6 (full meteorology) and Test Case 7 (no meteorology).

	Change in Flow Magnitude (m^3 s^{-1})	Change in Concentration Full Meteorology	Change in Concentration No Meteorology
Change in Flow Magnitude (m^3 s^{-1})	1		
Change in Concentration Full Meteorology	0.05	1	
Change in Concentration No Meteorology	0.48	0.34	1

Table 9: Correlation coefficient analysis for change in wind speed (m/s) and the change in particle concentration for Test Case 6.

	Change in Wind Speed (m/s)	Change in Concentration
Change in Wind Speed (m/s)	1	
Change in Concentration	0.10	1

Table 10: Correlation coefficient analysis for change in wind direction and the change in particle concentration for Test Case 6.

	Change in Wind Direction	Change in Concentration
Change in Wind Direction	1	
Change in Concentration	-0.02	1

Table 11: Correlation coefficient analysis for changes in east winds' velocity and the change in particle concentration for Test Case 6.

	Change in Wind East Velocity $(m^3 \ s^{-1})$	Change in Concentration
Change in Wind East Velocity $(m^3 \ s^{-1})$	1	
Change in Concentration	0.02	1

Table 12: Correlation coefficient analysis for changes in north winds' velocity and the change in particle concentration for Test Case 6.

	Change in Wind North Velocity $(m^3 \ s^{-1})$	Change in Concentration
Change in Wind North Velocity $(m^3 \ s^{-1})$	1	
Change in Concentration	-0.07	1

Table 13: Correlation coefficient analysis for flow conditions and model predicted residence, flushing, and exposure times.

	Flow Conditions (Cu. m/s)	Residence Time (days)	Flushing Time (days)	Exposure Time (days)
Flow Conditions (Cu. m/s)	1			
Residence Time (days)	-0.72	1		
Flushing Time (days)	-0.65	1.0	1	
Exposure Time (days)	-0.69	1.0	1.0	1

Table 14: Regression analysis of model predicted residence time and the magnitude of steady, riverine discharge.

RESIDENCE TIME

SUMMARY OUTPUT

Regression Statistics	
Multiple R	0.72
R Square	0.52
Adjusted R Square	0.36
Standard Error	24.43
Observations	5.00

ANOVA

	df	SS	MS	F	Significance F
Regression	1	1924.90	1924.90	3.22	0.17
Residual	3	1790.68	596.89		
Total	4	3715.58			

	Coefficients	Standard Error	t Stat	P-value	Lower 95%	Upper 95%
Intercept	54.56	15.87	3.44	0.04	4.07	105.06
Flow Conditions (Cu. m/s)	-0.01	0.00	-1.80	0.17	-0.02	0.01

Table 15: Regression analysis of model predicted exposure time and the magnitude of steady, riverine discharge.

EXPOSURE TIME

SUMMARY OUTPUT

Regression Statistics	
Multiple R	0.65
R Square	0.42
Adjusted R Square	0.22
Standard Error	47.15
Observations	5

ANOVA

	df	SS	MS	F	Significance F
Regression	1	4766.86	4766.86	2.14	0.24
Residual	3	6669.77	2223.26		
Total	4	11436.62			

	Coefficients	Standard Error	t Stat	P-value	Lower 95%	Upper 95%
Intercept	74.39	30.62	2.43	0.09	-23.07	171.84
Flow Conditions (Cu. m/s)	-0.01	0.01	-1.46	0.24	-0.04	0.02

Table 16: Regression analysis of model predicted flushing time and the magnitude of steady, riverine discharge.

FLUSHING TIME
SUMMARY OUTPUT

Regression Statistics	
Multiple R	0.69
R Square	0.48
Adjusted R Square	0.31
Standard Error	29.47
Observations	5.00

ANOVA

	df	SS	MS	F	Significance F
Regression	1	2,423.99	2,423.99	2.79	0.19
Residual	3	2,605.31	868.44		
Total	4	5,029.30			

	Coefficients	Standard Error	t Stat	P-value	Lower 95%	Upper 95%
Intercept	64.61	19.14	3.38	0.04	3.71	125.52
Flow Conditions (Cu. m/s)	-0.01	0.01	-1.67	0.19	-0.03	0.01

BIOGRAPHICAL SKETCH

BIOGRAPHICAL SKETCH

Name of Author: Christian D. Marr

Place of Birth: Heidelberg, Germany

Date of Birth: March 29, 1986

Graduate and Undergraduate Schools Attended:

University of South Alabama, Mobile, Alabama
University of South Alabama, Mobile, Alabama

Degrees Awarded:

Bachelor of Science in Civil Engineering, 2010, Mobile, Alabama
Master of Science in Civil Engineering, 2013, Mobile, Alabama

Awards and Honors:

CMES Scholarship Recipient, 2007
Dean's Honor List, 2007 – 2008
Research Assistant, 2008 – 2010
Graduate Research Assistant, 2011 – 2013
Graduate Teaching Assistant, 2012
Tau Beta Pi, Engineering Honor Society, 2012